The physics of paper. Rep Prog Phys

Article *in* Reports on Progress in Physics · March 2006

DOI: 10.1088/0034-4885/69/3/R03

2 authors:

Mikko Juhani Alava
Aalto University
399 PUBLICATIONS **7,934** CITATIONS

SEE PROFILE

Kaarlo Niskanen
Mid Sweden University
103 PUBLICATIONS **2,141** CITATIONS

SEE PROFILE

INSTITUTE OF PHYSICS PUBLISHING REPORTS ON PROGRESS IN PHYSICS

Rep. Prog. Phys. **69** (2006) 669–723 doi:10.1088/0034-4885/69/3/R03

The physics of paper

Mikko Alava[1] **and Kaarlo Niskanen**[2]

[1] Helsinki University of Technology, Laboratory of Physics, PO Box 1100, 02015 HUT, Finland
[2] KCL Science and Consulting, PO Box 70, 02150 Espoo, Finland

Received 3 May 2005, in final form 24 November 2005
Published 15 February 2006
Online at stacks.iop.org/RoPP/69/669

Abstract

Paper is a material known to everybody. It has a network structure consisting of wood fibres that can be mimicked by cooking a portion of spaghetti and pouring it on a plate, to form a planar assembly of fibres that lie roughly horizontal. Real paper also contains other constituents added for technical purposes.

This review has two main lines of thought. First, in the introductory part, we consider the physics that one encounters when 'using' paper, an everyday material that exhibits the presence of disorder. Questions arise, for instance, as to why some papers are opaque and others translucent, some are sturdy and others sloppy, some readily absorb drops of liquid while others resist the penetration of water. The mechanical and rheological properties of paper and paperboard are also interesting. They are inherently dependent on moisture content. In humid conditions paper is ductile and soft, in dry conditions brittle and hard.

In the second part we explain in more detail research problems concerned with paper. We start with paper structure. Paper is made by dewatering a suspension of fibres starting from very low content of solids. The processes of aggregation, sedimentation and clustering are familiar from statistical mechanics. Statistical growth models or packing models can simulate paper formation well and teach a lot about its structure.

The second research area that we consider is the elastic and viscoelastic properties and fracture of paper and paperboard. This has traditionally been the strongest area of paper physics. There are many similarities to, but also important differences from, composite materials. Paper has proved to be convenient test material for new theories in statistical fracture mechanics. Polymer physics and memory effects are encountered when studying creep and stress relaxation in paper. Water is a 'softener' of paper. In humid conditions, the creep rate of paper is much higher than in dry conditions.

The third among our topics is the interaction of paper with water. The penetration of water into paper is an interesting transport problem because wood fibres are hygroscopic and swell with water intake. The porous fibre network medium changes as the water first penetrates into the pore space between the fibres and then into the fibres. This is an area where relatively little systematic research has been done. Finally, we summarize our thoughts on paper physics.

(Some figures in this article are in colour only in the electronic version)

Contents

1. Introduction—the pedestrian view of paper

1.1. Why is paper interesting?

Most of the materials that one encounters in daily life contain interesting physics one way or the other. This is particularly true where paper is concerned. In the following review we present an overview of some of the intriguing phenomena that are encountered in the context of such 'fibre networks'. To us, the definition of paper physics emphasizes the statistical physics and materials science of paper. Such a starting point is fruitful given that the structure of paper is inhomogeneous [1]. We concentrate here on the role of disorder and how this influences the particular physical aspects of paper.

The use of paper in studies of phenomena in disordered media has found many applications. One of the first applications was the use of paper as a model material for the elastic modulus and strength of two-dimensional (2D) random systems. For example, very thin paper sheets (such as toilet tissues) correspond to 2D networks of springs close to a percolation threshold, or with central forces since the fibres are very thin [2]. At higher thicknesses, such as for ordinary office paper grades, the typical distance between adjacent inter-fibre bonds is equal to fibre width. In this case paper resembles a 2D random beam network and the basics of elasticity change [3].

The theory of random fibre networks (RFN) has recently resurfaced in another context, that of biological physics. While in paper the bond between fibres has to be considered 'rigid', so-called actine networks provide an example of RFN's with central-force contacts (spring-like) between crossing 'fibres' [4, 5]. This change, possibly also of interest for the elasticity of fibre assemblies in suspensions, implies profoundly different behaviour at small densities. The transfer of forces takes place via so-called rigidity percolation, which implies that for structural stiffness the force networks have to be more than 'one-dimensional'; one needs parallel force-carrying chains [6, 7].

Another interesting, recently studied case is the slow combustion front in paper; here the emphasis is on generic scaling laws for a propagating interface separating intact material from the burned part but not so much on the paper properties. Such a front is described by a one-dimensional profile $h(x)$, where h becomes a self-affine fractal. In this the paper structure plays a role by giving rise to a disordered environment [8–11].

Likewise, there are many experiments on fluids in porous media that have used a paper substrate to look at phenomena where a disordered structure is useful [12]. Later on we shall discuss the peculiar properties of fibre webs in the following kind of contexts: imbibition, fluid flow and swelling, separately and combined. These have practical uses also ranging from printing processes to packaging. Paper as a barrier material is again such that its dual nature comes forth: the pore space is now important, as it results in pathways for the passage and diffusion of gases and fluids [13–15].

In contrast to the preceding examples the electrical properties of paper are not related to the disordered structure but are quite sensitive to moisture. Paper is an insulator due to the intrinsic materials properties of the cellulosic fibres [16, 17]. However, its conductivity increases proportional to moisture content raised to power 9 [18]. The effect comes from ionic conductivity since the ion content of paper influences conductivity. Also the dielectric (ac) properties of paper depend on moisture content but not as much as dc resistivity. The electrical properties of paper are relevant because of 'laser' printing and copying, or electrophotography. In this process the print is formed by toner (ink) particles that are transferred on the paper surface by an electrical field. The process relies on the resistivity and polarizability of paper. Differences in air humidity influence paper performance in this process, making it difficult to optimize paper [19].

Table 1. Characteristic properties of softwood fibres used in papermaking.

	Mass per unit length ($mg\,m^{-1}$)	Length (mm)	Width (μm)	Basis weight ($g\,m^{-2}$)
Scots pine (springwood)	0.16	2.1	37	4.3
Scots pine (summerwood)	0.31	2.1	30	10.3
Western hemlock	0.20	2.4	31	6.5
Douglas fir	0.25	2.8	34	7.1

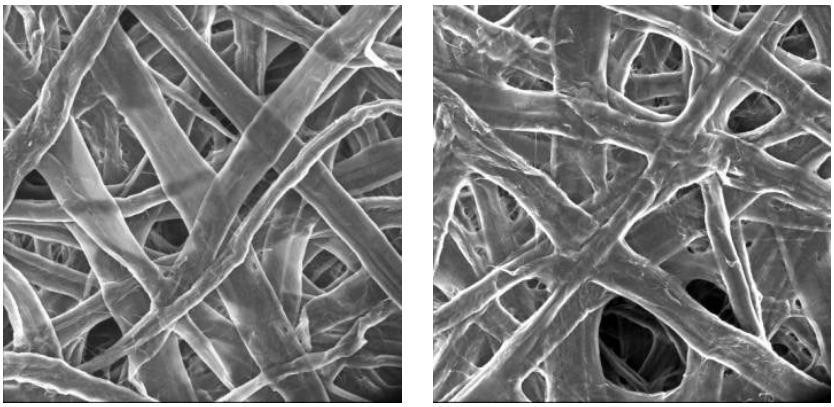

Figure 1. Scanning electron microscope image of a paper surface (KCL). Two cases, paper dried under tension (top) and free of tension (bottom), are shown.

1.2. What is paper made of?

The most important ingredients of the final product are cellulosic fibres, made from wood or other similar natural origins and the pore space formed by and in between the fibres. Typical everyday papers contain fibres that are made by separating them in an industrial manufacture process by mechanical work (mechanical pulp) or by cooking (chemical pulp). Typical dimensions are listed in table 1. The key characteristic of fibres is their length, a few millimetres as a rule. Fibre manufacturing—the separation of fibres from wood—frequently damages the fibres. This is especially true for mechanical pulp where the majority of particles are broken fibres and fibre fragments [20].

The origin of the inhomogeneity in paper lies in the sheet forming process. The process involves turbulent flow of a suspension of water and fibres, its filtration and sedimentation on a wire. Industrial paper has, due to its anisotropic origin, two principal directions, the 'machine direction' or along the wire (MD) and the 'cross direction' or CD. The mass fraction of fibres in the fibre suspension is ca 1% initially. It increases to ca 20% at the end of the drainage process. At this point fibres and the other constituents of paper can no longer move freely relative to each other. Further water is removed by pressing and evaporating.

The stochastic nature of the drainage process leads to a planar network structure where the positions, orientations and shapes (i.e. curl, kinks, undulations, etc) of the fibres are random (see figure 1) [21]. After drainage, the paper structure has correlations, which influence transport properties including, in particular, the optical ones. The important quantity is the remaining mass per unit area, in engineering language by basis weight, in units of grams per square metre (see table 1 for the basis weights of typical fibres). In commercial paper grades technical properties are controlled by a carefully optimized combination of appropriate pulp

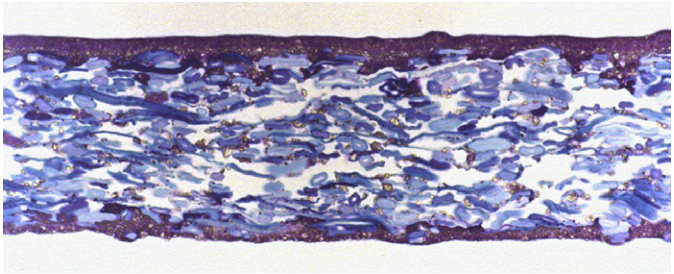

Figure 2. Cross-sectional image of a coated paper sheet. The thickness is of the order of 0.1 mm (KCL).

fibre types and other constituents. Paper can be coated by a layer of mineral particles, and the 'bulk' can contain similarly small-scale fillers that act to change the porosity and the optical properties. In the process of drainage the fibre fragments, mineral fillers, colloids and many polymeric additives are retained at random locations on the fibre surfaces. This randomness at micrometre-scale adds to the complexity of the random fibre network.

High quality printing papers are always coated (see figure 2). Since we will not dwell on the coating layer structure elsewhere in this review, a brief account is in order. The coating layer improves the uniformity of the paper surface and reduces the characteristic pore sizes from tens of micrometres for/at uncoated paper surface to fractions of a micrometre. This happens simply because of particle dimensions. If one considers the planar packing of relatively stiff fibres with the packing of spherical filler particles, it becomes clear that one should crush fibres to achieve a smooth surface on a fibre network.

The process of paper coating is analogous to the filling of holes in a wall before painting. Also in paper coating the 'plaster' is a rather viscotic water-based paste that is sheared on the paper surface with a blade. The consolidation of the coating paste takes place through colloidal and surface tension forces. Latex binder keeps the coating particles together, just as in ordinary latex paint. Qualitatively the consolidation of paper coating resembles the drying of sand (see [22] for simulations). Several kinds of particles are often present in the coating layer. One may consider analogies to 'Apollonian packings', or, more generally, to granular materials, to study the effect of the particle size distribution on the porosity of the final packed state or other properties [23]. The same also applies to the effect of various compactification procedures [24].

1.3. Paper structure and optics

The optical properties of paper are very sensitive to its structure. An important qualification of printing and writing paper grades is opacity. Opacity is necessary so that one can read the print or writing on one side without interference from the other side. Opacity arises from the scattering of light from free surfaces in the sheet, the surface layers (or coating layer), fibre surfaces and filler surfaces. Industrially manufactured filler particles, such as precipitated calcium carbonate (PCC) have a high specific surface area to enhance opacity.

For the optical properties the most important structural property is the number of pores along the photon flight path, such that the pore thickness exceeds half the wavelength of light, say 200 nm. This length scale can be compared with the thickness of a typical paper, 100 μm, or the thickness of a typical papermaking fibre, 5 μm. Almost all printing and writing papers contain at least ten light-scattering layers in the thickness direction [25].

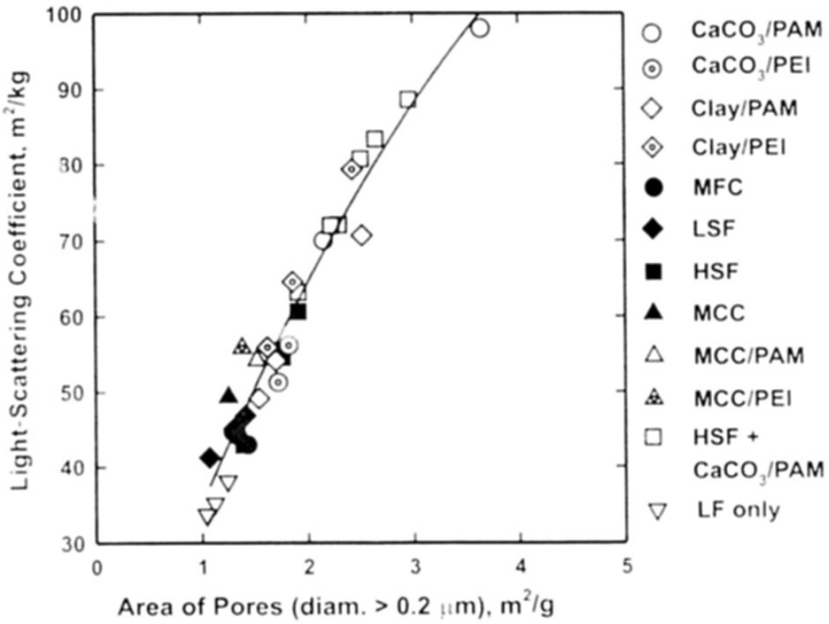

Figure 3. Light scattering coefficient against specific pore area for papers made of different types of fibres and filler particles [29].

A simple question that is hard to answer is how the manufacturing process and constituents of paper influence the pore structure of paper. Obviously much of the fibre surface area must be bonded to other fibre surfaces in order to have a solid sheet instead of loose fibres. The fraction of the surface area that takes part in this is called the relative bonded area (RBA). Most of the pores in paper are small, close to the the optical scattering limit. The pore size distribution is naturally continuous at that length scale since all the particles, fibres, fibre fragments and fillers have rough surfaces. One-dimensional ray optics (Kubelka–Munk model) with phenomenological scattering and absorption coefficients have been traditionally used to characterize paper optics. However, the effects of tailor-made optical filler materials, in particular, cannot be explained without numerical simulations of multiple scattering [26–28].

The index of refraction of most papermaking materials is 1.55, relatively close to that of water, 1.3. This explains, as everyone knows, why paper loses most of its opacity upon water application. Inversely, the reduction in opacity can be used to measure the penetration rate of water into paper. The uniformity of the index of refraction implies that the free surface area controls the light scattering coefficient of paper (figure 3). Indeed, the total surface area of pores larger than 200 nm, as measured with mercury intrusion, is linearly proportional to the light scattering coeffient, irrespective of the composition of paper [29].

The small thickness of paper (typically ten layers of fibres) complicates the study of the network structure. A large fraction of fibre layer belongs to the surfaces that, according to the sedimentation analogy, have a structure different from that of the bulk interior. Even the definitions of thickness and porosity of paper require care. The point-wise mean distance between the top and bottom surfaces naturally gives a minimum for the sheet thickness that depends on the in-plane resolution. The corresponding porosity value is a lower bound that does not agree with the porosity measured inside the sheet [30].

Yet another feature revealed by paper opacity is the ‘cloudiness’ of paper. The millimetre-scale inhomogeneity is clear if one looks through any sheet of paper against a lamp (as long as

the opacity is not so high that no light comes through). It arises from the areal mass variations of the basis weight. The simplest imaginable procedure to create a sheet is to have a very dilute suspension of fibres in water and to drain it slowly from the container or to let the fibres settle at an infinitesimal rate. This gives rise to Poissonian statistics. Real paper is different: its cloudiness reflects the flocculation of fibres that takes place during drainage. Fibres form flocs in the suspension due to a variety of attractive forces: electrostatic, colloidal and mechanical if in close contact. A fibre suspension, if left to settle, will form a grainy, porridge-like substance. The flocculation process deals with random geometry starting from percolation, and with such statistical physics concepts as aggregation and clustering. Hydrodynamics and the mechanics of fluid–particle systems also play a large role [31].

In practice the uniformity of mass distribution is the most important property of paper. Much of the effort in the development of papermaking has gone into reducing it. Cloudiness influences not only the visual impression of the paper itself. Since paper is pressed between rollers in the manufacturing process, the areal mass distribution affects the density and surface pores of the fibre network. This in turn affects the uniformity of print on uncoated papers and the structure of the coating layer in coated papers. Strong mass variability can imply strength problems. If moisture content increases, a more 'cloudy' paper loses its flatness more easily than a less 'cloudy' paper. Everyone knows what happens to a book if it gets wet. Afterwards, the cockled shape of the pages is a reflection of the 'cloudiness' of the paper structure.

1.4. Mechanical properties

The presence of two intertwined 'phases'—fibres and the pores—gives rise to interesting analogies to composites and granular media. An example of this is the elasticity of these materials. In both cases the fundamental questions resemble those that one meets in paper mechanics: how is the stress transferred from one fibre to another—in fibre-matrix composites this happens via the matrix. And, what kind of 'force networks' does exist? (For a recent paper concerning this in the case of frictionless grains as an analogy , see [32]). Or, one can simply ask how paper crumbles [33, 34], as a basic problem of the discontinuity or ridge formation in quasi-two-dimensional elastic media.

An obvious but simplified analogue of the papermaking process comes from the physics of the kitchen: the 'network geometry' spaghetti resembles paper if drained and allowed to dry out on a flat surface. Also the spaghetti strands bond together with hydrogen bonds. However, an important difference between a dried spaghetti network and paper comes from the helical internal structure of wood fibres that are used in papermaking [35].

Before continuing the discussion, we must complete the description of the papermaking process. After the drainage phase, the planar fibre network is held together by surface tension forces, giving it viscoelastic character. After this the sheet is first pressed between rollers and then heated with hot cylinders to remove the remaining water. In this process, the water menisci between fibres shrink pulling fibres against one another so that hydrogen bonds can form at the molecular contact between adjacent fibre surfaces [36, 37]. The inter-fibre bonds are the factor that controls, in one way or other, all the mechanical properties of paper [38].

In the wet state the helix of the fibre wall is swollen, more in the transverse direction than in the axial direction of the fibre. When paper is dried, the anisotropic shrinkage leads to internal stresses in the fibre network because the axial stiffness of the fibres resists the transverse shrinkage tendency. This phenomenon is very important for the mechanical properties of paper, as we will discuss in section 3.

The comparison of different papers easily reveals how much the mechanical properties of paper can vary. Tensile strength, elastic stiffness and fracture toughness are useful properties

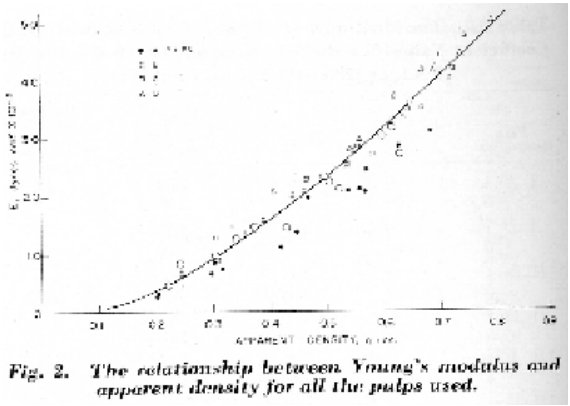

Figure 4. Elastic modulus against density. The changes were obtained by beating the fibres mechanically. This treatment opens up the fibre wall structure and leads to a denser sheet structure [39].

in printing processes and packaging applications. High bending stiffness (i.e. rigidity) is necessary for easy handling of office paper sheets and magazines. Sack paper must be tough while a dense grease-proof paper is unavoidably brittle. Tissue paper has a very open and sparse structure, a necessity for ductility and softness (figure 4).

The elasticity of fibre networks is a surprisingly tough a problem, with apparent analogies to percolation theory, composite mechanics and to fibre reinforcements in composites. These tempting analogies are in fact misleading. The elasticity of most papers is not related to a percolation problem: the inter-fibre connectivity is roughly an order of magnitude above the percolation threshold. Tissue papers are the only exception. The composite picture is unrealistic because there is no separate matrix phase in paper—fibres are the only continuous solid phase. Paper is more complicated than a fibre reinforced material because, as we will discuss below, the mechanical properties of the fibres in paper depend on the network which they have dried into. This is the load carrying part of a fibre between two neighbouring contacts to other fibres, that is, any two subsequent bonds along the fibre. Should one be able to compute its elastic energy, the problem would be solved. Unfortunately the geometry is random, thus a 'typical' segment is hard to define as also the character of the stress transfer between fibres.

The same complications exist in the context of fracture [40] and irreversible deformation. Runnability, the ability to use a paper web in a printing press with the least amount of web breaks, relates to this issue. This is a classical branch of engineering mechanics where it is understood as a problem of extreme statistics—what is the typical tensile strength of a sample of size L and its distribution? Lately the statistical physics community has been able to contribute to such issues by using simplified models opening up an interesting connection [41].

One can do a hand-test by tearing a piece of paper apart, which touches upon two intriguing statistical aspects and a practical one: the crack surfaces produced by a paper fracture experiment are 'rough', that is they can be described with self-affine geometry. At the simplest level, this implies that the mean-square width of the fracture surface increases as a power-law of the observation window size similarly to many engineering materials. Paper is rather unique since in this context it is effectively two-dimensional [42]. Why rough cracks are formed is little understood, on the level of fundamental laws, and the issue contributes an active, lively subfield of non-equilibrium statistical mechanics.

The practical question also is how to understand the crack surface energy in paper, a tough job due to the disordered structure. The average energy spent in forming cracks is related to the

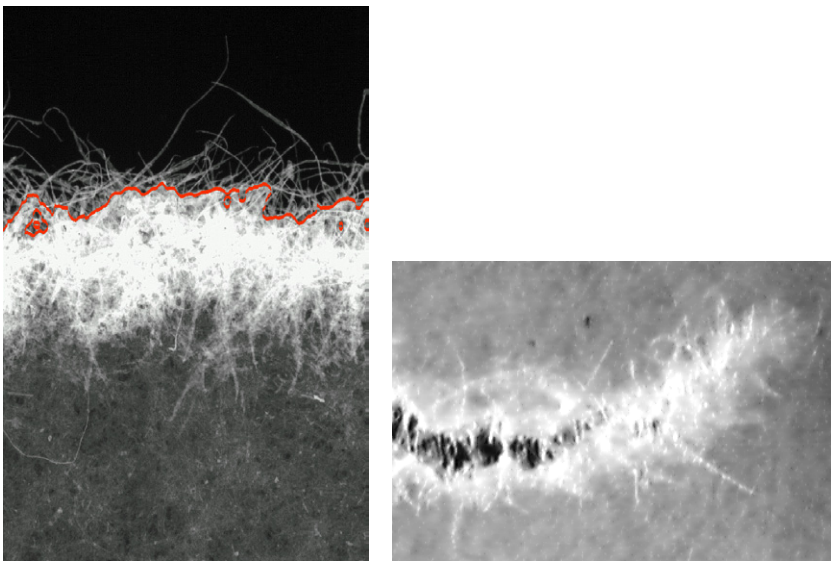

Figure 5. Fracture process zone in paper made visible by impregnation with a silicone that has been cured before the fracture test. The silicone fills all the pores in paper, hence rendering it translucent. In the failure process, inter-fibre bonds open. This creates light-reflecting surfaces. The first panel illustrates the continuous nature of the damage zone in paper fracture: the residual areal density varies continously between zero and the bulk - and individual fibres stick out (indicating the scale to the image). The second panel shows the 'cloud' of damage at a crack tip on a slightly larger scale. In particular, it is evident that the fracture process zone is rather large and diffuse and extends well ahead of the region where noticeable microcracks or voids can be seen [44].

concept of fracture toughness, that in the engineering literature has for decades been defined by the Griffith criterion. Paper combines two aspects, disorder and the polymeric nature of the cellulosic material, in an intertwined way, which influence the fracture properties. It would also be interesting to understand the fast fracture of paper, a topical problem in other contexts due to its many unresolved facets (see e.g. [43]).

The second curious phenomenon is the 'crackling noise' [45] that arises in the fracture and which one can also partly hear directly. This is another example of a (non-equilibrium) stochastic process, and the acoustic events follow power-law probability distributions. What the relation of this observation is to the paper structure, to the dynamics of rough cracks and to fracture toughness is again wide open but the same can be stated also in other contexts in which similar signatures of the statistical nature of fracture processes can be observed such as rocks, concrete, fibre composites, wood, etc [46–50]. See figure 5.

Water breaks hydrogen bonds so that fibres can slide against one another. In general, wet paper has lower strength and lower stiffness than dry paper. Paper grades (say kitchen tissue) that are used in wet conditions contain chemical bonding additives that increase the wet strength. Other paper grades lose strength and stiffness and become ductile when wetted, as one can easily observe.

1.5. Effects of water in paper

Wood fibres are hygroscopic—they absorb water readily. Thus the interaction of paper with water-based liquids is inherently complicated. One can consider this on various scales from the microstructure of fibres to the penetration of water into disordered pore networks.

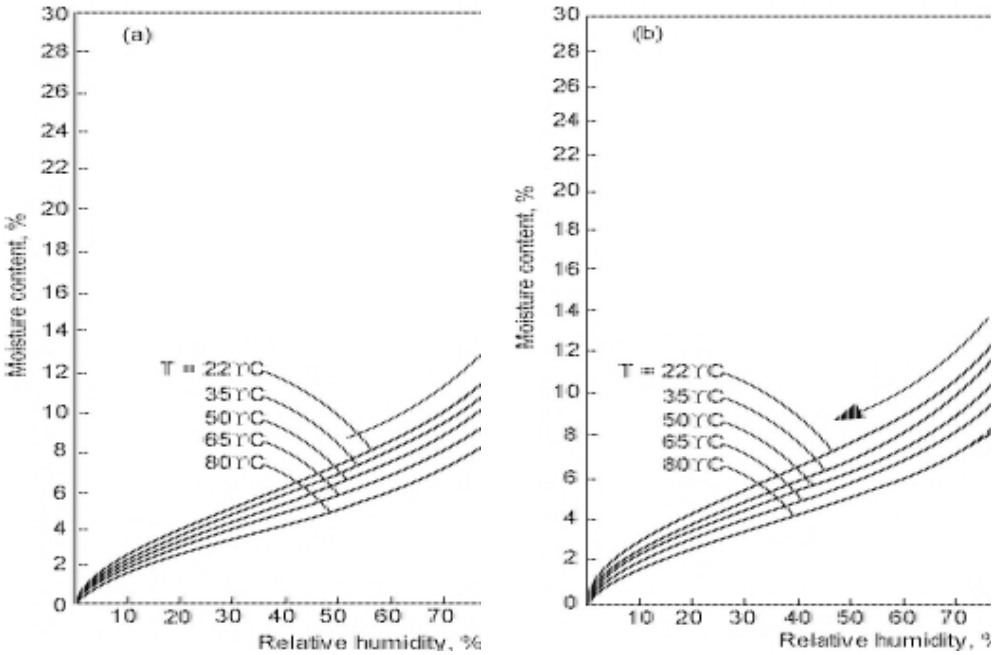

Figure 6. Moisture content of paper at different temperatures when the relative humidity of ambient air is varied ([51]).

The moisture content of paper is the ratio of absorbed water divided by the mass of oven dry paper. When in equilibrium with the surrounding air, the moisture content of paper depends on the relative humidity of air and the equilibrium temperature and can be formulated via the appropriate thermodynamic relationships [51].

The moisture content decreases with increasing temperature or with decreasing relative humidity as figure 6 shows. There is a slight hysteresis in the moisture content at a certain relative humidity of air depending on whether one starts from humid or dry conditions. A pair of boundary curves determine the lowest and highest moisture content that paper can have at a given relative humidity. Intriguingly, depending on the humidity history, the actual content can lie anywhere between these [52].

The hygroscopic nature of papermaking fibres influences the behaviour of paper if the moisture content changes. With increasing air humidity paper swells and with decreasing air humidity it shrinks. The dimensional changes are fractions of a per cent and therefore difficult to see with the naked eye. However, the effect can be readily observed by exposing only one side of a paper sheet to a moisture change. Very simply, one can just blow on a paper strip and see how the moisture in one's breath swells the exposed side of the strip, causing it to curl away. In a minute or so the strip will bend back as homogeneous moisture distribution is recovered. The phenomenon observed in such an experiment is called paper curl. It is a nuisance, for example, in copy machines where the print is fixed by heating. This leads to evaporation, hence curl and eventually paper jams inside the machine.

Two more interesting curl phenomena can easily be observed. First, if the one-sided moisture exposure is high enough, the resulting curl will recover *beyond* the original state. For example, if one wipes a little liquid water on one side of a paper strip, the strip will at first rapidly assume a curved shape with the wet side outwards. However, after a while the curvature changes direction, and in the end an initially flat strip will display curvature towards

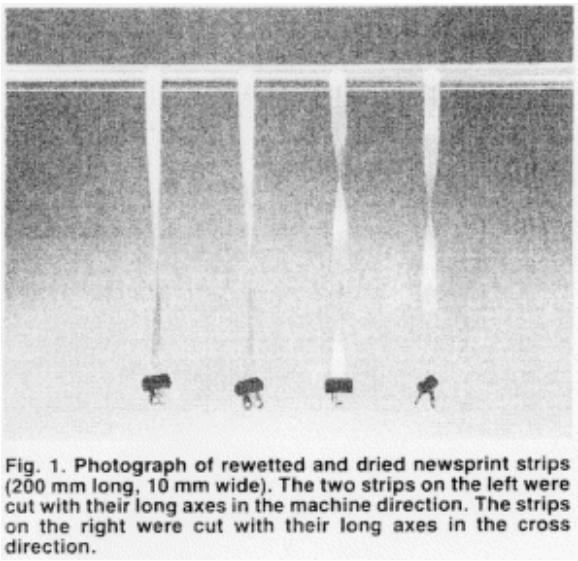

Fig. 1. Photograph of rewetted and dried newsprint strips (200 mm long, 10 mm wide). The two strips on the left were cut with their long axes in the machine direction. The strips on the right were cut with their long axes in the cross direction.

Figure 7. Paper strips cut from printing paper twist when the moisture content changes (from [53]).

the side on which water was applied. The origin of this peculiar phenomenon lies in the high creep rate of wet fibre networks. The dry side of the paper resists the expansion of the wet side. This leads to compressive creep in the wet side of paper, which therefore remains shorter when the moisture has evened out.

The second interesting aspect of curl is chirality. It turns out that all wood fibres have the same right-handed chirality in their helical structure. When the moisture content of wood fibres changes, all fibres twist in the same direction. This chirality translates into chiral curl of paper. If one takes any flat sheets of paper and, for example, dries them in a microwave oven, the resulting curl is right-handed in all the sheets. Sheets cut out of newspaper are best for this experiment because the heat-induced curl in that paper grade is permanent (figure 7).

Papermaking fibres absorb water in two (or four) ways: (i) free water goes to the pores between fibres and as intra-fibre free water in the lumen of fibres, (ii) bound water gets either frozen to the pores of fibre walls or chemically bonded to the hydroxylic and carboxylic acid groups in fibres.

The chemical composition of the pulp affects swelling since the swelling water attaches to hydroxyl groups [54]. Cellulose and hemicelluloses contain more of these per carbon than lignin. Also, the group should be available for bonding, which is less true for crystalline cellulose than amorphous semicellulose. At room temperature, the saturation moisture content is characteristically 10% in lignin, 30% in cellulose and 80% in hemicellulose [55].

The hygroexpansivity of paper comes from the swelling or contraction of fibres when their moisture content changes. Over the range of RH from 0 to 100% at room temperature, the cellulosic fibrils expand approximately 1% in the longitudinal direction of the fibrils and approximately 20% in the lateral direction [56]. The corresponding hygroexpansion coefficients of the fibre reflect this: the fibres swell more radially than longitudinally and as a result the macroscopic network, paper, expands. Uesaka and Qi have computed the hygroexpansion coefficient(s) β of paper in the machine and cross-machine directions, which turn out to be dependent on the transverse and axial hygroexpansion of fibres [57]. Their relative importance depends on the inter-fibre bonds and their three-dimensional (3D) nature.

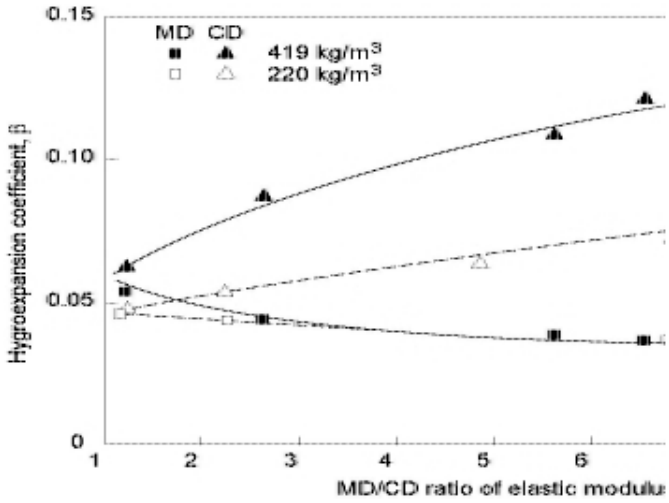

Figure 8. Effect of fibre orientation on the hygroexpansion coefficient, β, in MD (squares) and CD (triangles) versus the MD/CD ratio of elastic modulus for freely-dried handsheets with anisotropic fibre orientation for unbleached softwood (kraft) pulp at two density levels, changed by wet pressing [58].

Figure 8 corroborates this theory, since increasing paper density had practically no effect on the β in the machine direction, where the bonds are conceiveably such that little of the fibre hydroexpansion is translated into that of the sheet. In CD, the situation is different because the transverse shrinkage of fibres can pull the entire sheet together during drying, which increases β. All in all, the response to moisture conditions is an amusing example of how the bond-level geometry of paper fundamentally affects its behaviour and provides a specific example of how the physical property of paper is determined by *average properties* and not ruled by disorder.

If the external conditions suddenly change, the moisture content of paper or board cannot change immediately to reflect this: the dynamics is governed by moisture diffusion. Diffusion times should therefore generally be proportional to thickness squared or basis weight squared, since the distance to the surface is important. This holds at relatively high basis weights. The diffusion time of moisture into paper is however linear at low basis weights [56, 59]. This is characteristic of a boundary layer formed at the sheet surface. In the boundary layer the local humidity and temperature differ from the ambient conditions, and particularly so that the boundary condition for the bulk diffusion becomes time-dependent [59, 60].

2. Structure of paper

A typical paper sheet contains, on average, ten fibres in the thickness direction. The fibre length is more than ten times larger than the sheet thickness. Thus a 'two-dimensional random fibre network' approximation is good for many purposes. Of the above ten typical fibres, roughly half are at some points exposed to the open sheet surface. The rest are completely with in the interior bulk structure. The local network structure there generally has lower density than the surface layers. In a laboratory one can increase the number of fibre layers and change fibre properties in order to obtain the analogue of a growth model or process that exhibits the transition from a two-dimensional to three-dimensional (3D) structure [61]. This picture is very powerful in the analysis of the optical properties of paper for example.

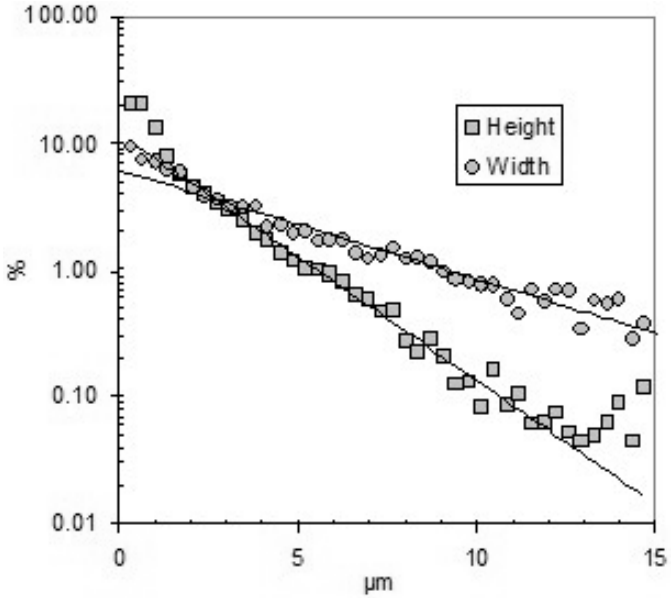

Figure 9. Distribution of free span in the planar and thickness directions of paper, measured from cross-section images. Note that the distributions are both exponential. Many interesting physical properties of paper depend on, say, the small height-part of the distribution (KCL).

2.1. Two-dimensional random fibre networks

Ideal fibres are long compared with their diameter. Their length controls their mass. The measurement of fibre mass per unit length is routine in papermaking. The two-dimensional random fibre network is thus characterized by the fibre length and either the number or mass of fibres per unit area. The mass per unit area is the RBA mentioned earlier, also called the grammage of paper. Typical numbers for basis weight range from $40\,\mathrm{g\,m^{-2}}$ for newspapers to $80\,\mathrm{g\,m^{-2}}$ for office papers.

Theoretical models employ total length per unit area as the measure of 2D network density, q. Using the typical basis weight numbers and fibre masses per unit length (table 1) indicates that the two-dimensional fibre density of real papers ranges from $q = 200$–$400\,\mathrm{mm\,mm^{-2}}$. In other words, there are 100–200 fibres in every square millimetre of paper. In such a random fibre network the mean distance between nearest neighbour fibre crossings, i.e. mean fibre segment length, is $2/q\pi$ [62].

This implies that if real papers were two-dimensional, the inter-fibre 'pores' or open areas in the sheet's plane would be a few micrometres in mean diameter. This would be an order of magnitude less than the typical width of real fibres and closer to the typical thickness of real fibres (table 1). Microscopic measurements of real papers indicate that the surface pore diameters are between the two-dimensional approximation and fibre width. An example of the 'lacunarity' or the distances between fibre surfaces inside pores is shown in figure 9.

In the 2D limit, the areal density q acts as the control parameter for percolation, cluster formation, etc. This is as usual a geometry problem, with some flavour added since the process takes place in a continuum, contrary to normal lattice percolation problems. The transition is characterized by the 2D percolation threshold, $q_c \simeq 5.7/l_f$ (where l_f is the mean fibre length) [63]. The threshold is dependent on the width of the fibres, so that q_c is a function

of the fibre aspect ratio: naturally wider fibres overlap more easily. The transition is second-order and has the usual 2D percolation critical exponents. Where this might change is if one assumes correlations in the locations of fibres. The critical thresholds of similar continuum percolation problems are often approximated by what is called the 'excluded area/volume' approach, which in this case is relevant, e.g. if one wants to understand in detail the behaviour of q_c as a function of the aspect ratio [64, 65].

In terms of the conventional basis weight units the percolation threshold q_c corresponds to 0.5–1 g m^{-2}, depending on the type of papermaking fibres. Typical papers (magazines, copy paper, etc) have thus a 100 times higher basis weight. Even though the two-dimensional approximation overestimates the connectivity of the real fibre network in paper (since all fibres whose 2D projections cross cannot connect to each other), it is clear that ordinary papers are far above the 2D percolation threshold. Thus percolation bears no relevance to the mechanical properties of paper for example, perhaps with the exception of very thin papers such as fancy tissues.

2.2. *Fibre-to-fibre correlations in mass distribution*

The starting point is to understand that real paper is a random structure, with a Poisson mass distribution so that the standard deviation - say in the areal mass measured point-wise - equals the square root of the mean. In real paper this is not true due to two phenomena, non-uniform fibre orientation distributions and, in particular, flocculation.

Flocculation refers to the aggregation of fibres, in the suspension, into clusters. In the context of paper physics this is often described by a crowding number C which is defined as the mean number of fibres, in the suspension, inside a spherical volume of diameter l_f ([66]). Laboratory experiments show that strong flocculation begins when C grows to 60. This happens to correspond to the consistencies used in real paper machines. This fact makes sense because although the efficiency of papermaking increases with consistency (less water to remove), one cannot accept a very nonuniform paper structure [67].

A general analogy for the formation of clusters is given by the statistical mechanics cluster–cluster aggregation models, and of these by the diffusive version, DLCA, for example, where clusters diffuse and join upon collision, and the reaction-limited version RLCA where the sticking probability is usually taken to be a small constant. In fibre suspensions, floc formation is controlled by geometric constraints and therefore by consistency, fibre length and fibre flexibility, and by fibre interactions such as colloidal, electrostatic and frictional forces. Simulations by the group of Klingenberg at the University of Wisconsin demonstrate clearly that flocculation stops if the flexibility of fibres increases or their friction decreases [68, 69].

The understanding of floc formation is still at its infancy. It could for instance be tackled similarly to the usual aggregation phenomena via the Smoluchowski equation, a mean-field cluster-density description of the process including aggregation and break-up of clusters and flocs.

The effect of flocculation on the mass distribution of a paper sheet depends on how the sheet is made. A simple drainage-based laboratory sheet mould will transport the flocs onto a collecting wire mesh. This implies already the existence of a filtering mechanism: obviously those parts of the formed deposit of fibres that have less flocs/fibres per unit area will have a smaller local permeability. This leads to a smoothing mechanism since less-dense areas will tend to accumulate more mass relatively. Such an effect has been demonstrated experimentally, in that, the local mass fluctuations get diminished from the Poissonian prediction [70].

In an industrial, 'fast' papermaking process shear forces and turbulence are applied in the drainage process in order to break emerging fibre flocs. Turbulence is a double-edged

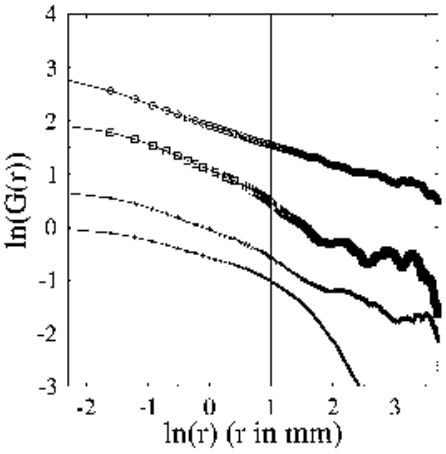

FIG. 2. A log-log plot of the correlation function $G(r)$ for four paper sheets of basis weights 7.2 g/m^2, 70.4 g/m^2, 86.3 g/m^2, and 118.9 g/m^2 (from top to bottom). The vertical line indicates the average fiber length $\lambda_3 = 2.7$ mm. Data are from set A, and the curves have been shifted for clarity. For the lowest densities, the power law extends up to about 14 times the fiber length.

Figure 10. An example of the $C(r)$ as measured from laboratory sheets. Notice the slow, power-like decay versus r (doubly logarithmic axis) [73]. Why this shape and not an exponential, for example?

sword in this respect since light turbulence breaks no flocs, but heavy turbulence increases inhomogeneity. Different spontaneous instabilities may also appear in the forming process. This is easy to understand because on a typical paper machine the fibre suspension is sprayed from a 10 m wide and 20 mm high headbox slice opening at the speed of 30 m s^{-1}. Vortex tubes for example, may appear and show up as streaks in the paper structure [71].

In both laboratory and industrial papers, an interesting question is how correlated the basis weight becomes if measured as a 'random point field'. In the former case due to the fibre orientation symmetry one can consider simply the two-point correlation function of the areal density, $C(r) = \langle \delta m(x) \delta m(x+r) \rangle$, where the average is taken over all x, and δm is the local deviation from average basis weight. In the latter case one needs to consider at least the MD and CD directions due to the 'symmetry breaking' or compute the radial dependence as well. Such an analysis is routinely used in troubleshooting. One can relate deviations from randomness with turbulence length scales [72].

If the paper structure were a Poissonian collection of flocs from a fixed probability distribution, $C(r)$ would reflect directly the assumptions of the floc sizes and of their internal structure versus the size [21]. Or, one can then assume that the flocs are deposited as a sheet so as to also maintain correlations in their positions, as is implied by the filtration mechanism [74]. Empirical observations reveal strong correlations in the basis weight up to a scale of several millimetres (figure 10). This is beyond the simplest floc scale. However, systematic studies on these correlations as a function of the degree of flocculation or educated guesses about their true origin are still missing. The formation includes texture from the correlation of the flow field and implies indeed cloudiness. See figures 11 and 12. Here, a basic question presents itself: it is obvious that there can exist several measures that each present the best choice for e.g. accounting for the physics of the formation or for relating to the end-uses (printing).

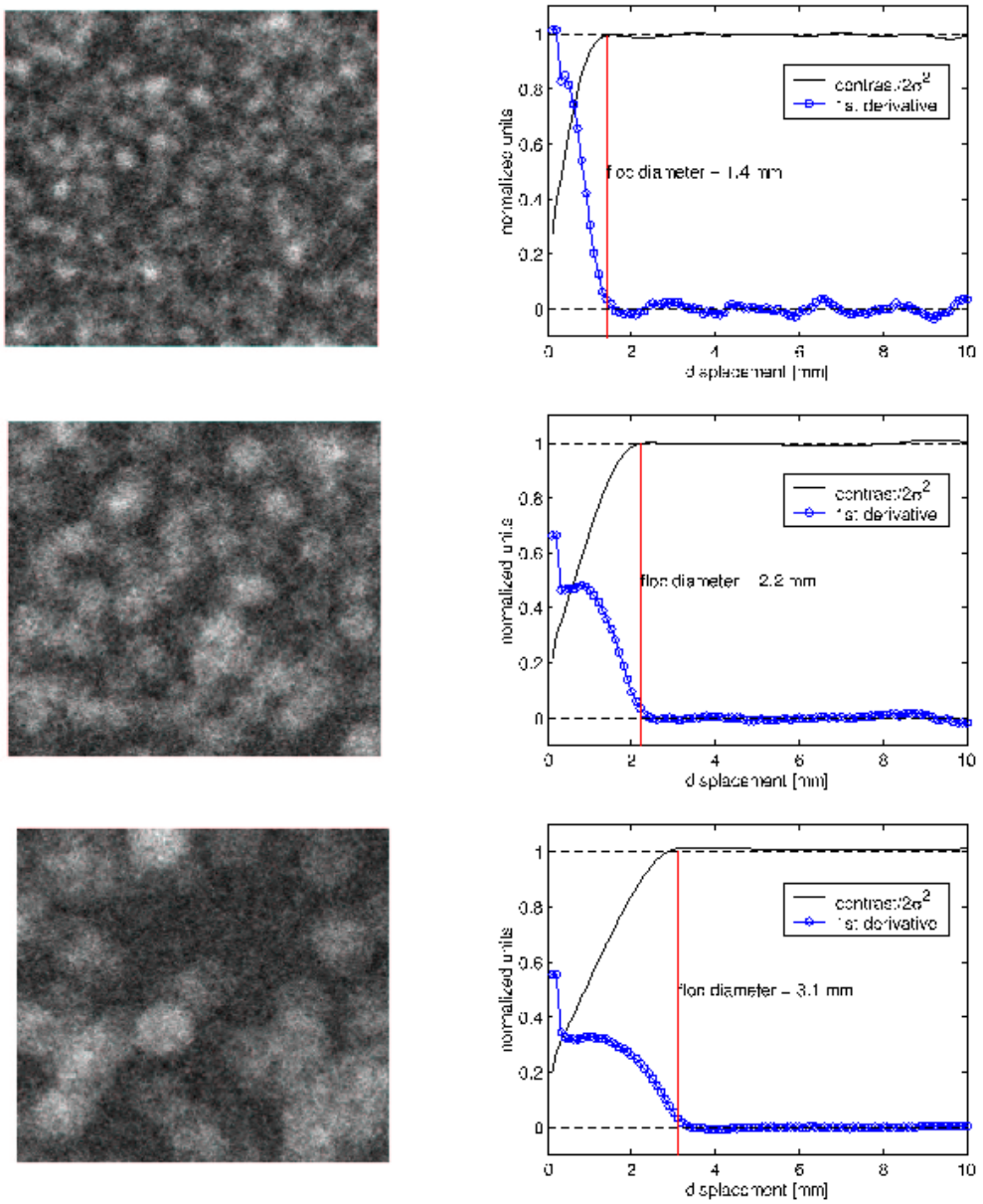

Figure 2. Left: grammage map, right: normalized contrast $C/2\sigma^2$ as a function of displacement in x direction of the image. Fiber length was l=1mm and diameter of elementary floc d=l (top), d=2l (middle) and d=3l (bottom).

Figure 11. Examples of 'flocculation' from grammage maps. The floc sizes as determined are in the right panel. Compare these with the appearance of the grammage. Courtesy M Kellomäki ([75]).

During the drainage process, shear forces orient fibres. For a dilute suspension of rigid fibres in a laminar shear flow, the fibre orientation distribution would be elliptical, instead of an isotropic or a symmetric 'circular' one. Fibre interactions and fluctuations in the local shear field cause deviations, resulting in interesting orientation distributions (figure 13). The origin

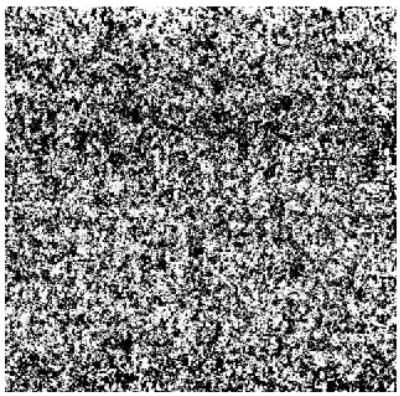

Figure 1. Median thresholded (black = high grammage) grammage map of sample 10A (c.f. Table 1) with "sharp" formation. Texture parameter values: $S = 2.72$ mm^{-1}, $d_C = 1.39$ mm and $C_{cl} = 0.028$.

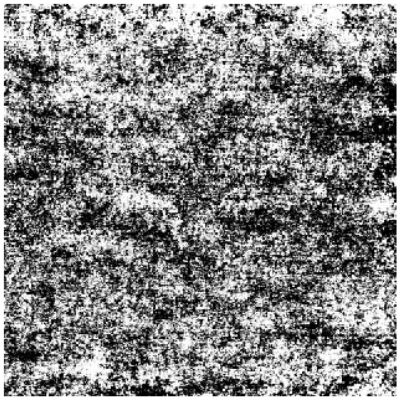

Figure 2. Median thresholded (black = high grammage) grammage map of sample 10E (c.f. Table 1) with "cloudy" formation. Texture parameter values: $S = 3.14$ mm^{-1}, $d_C = 2.42$ mm and $C_{cl} = 0.111$.

Figure 12. An example of the texture due to formation in paper. What would be mathematically the best way to characterize the 'graininess'? [76].

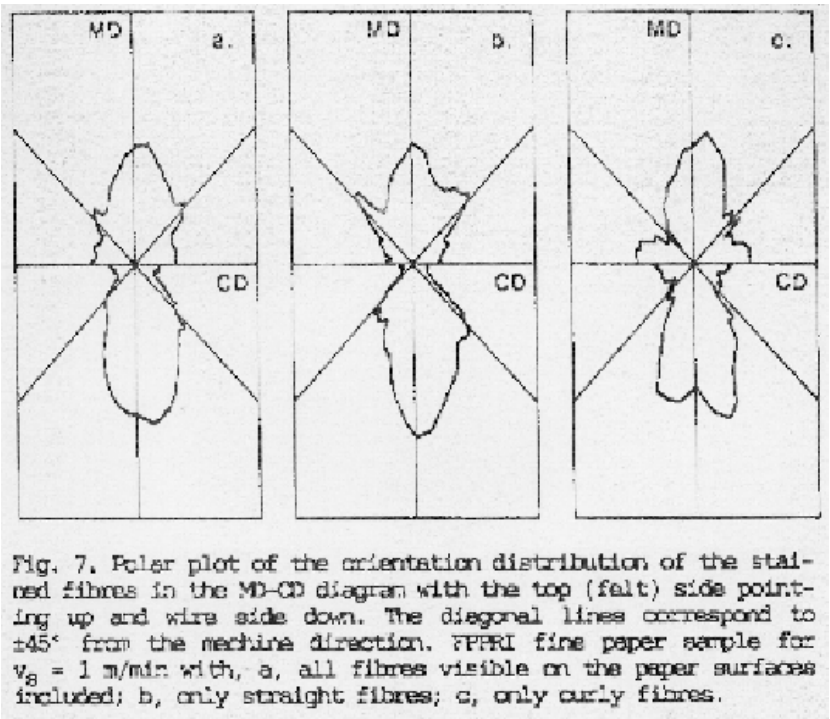

Fig. 7. Polar plot of the orientation distribution of the stained fibres in the MD-CD diagram with the top (felt) side pointing up and wire side down. The diagonal lines correspond to ±45° from the machine direction. PPRI fine paper sample for v_s = 1 m/min with, a, all fibres visible on the paper surfaces included; b, only straight fibres; c, only curly fibres.

Figure 13. Distribution of fibre orientations in the plane of paper. A small number of dyed fibres were added in the sheet for the micoroscopic measurement [77].

of the 'horns' is not certain but it is suspected that it arises from fibre interactions that prevent the free rotation of fibres [77].

Shear forces arise from spatial variations in the flow field, which in turn cause mass fluctuations. Thus there must be correlations between local mass and local fibre orientation.

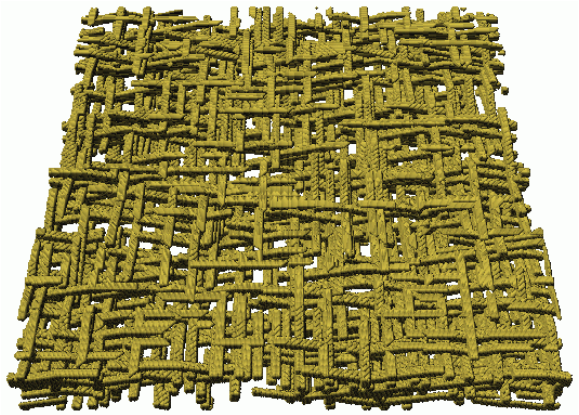

Figure 14. An example of a 2D fibre network constructed with the 3D fibre deposition model. The porosity of the network is about 0.83. The model is that of [61].

In simple terms, the gradient of mass distribution should be connected with the anisotropy of fibre orientation. The problem is complicated by the temporal fluctuations of the flow patterns during the drainage process. Hence the local orientation varies also in the thickness direction.

2.3. Ideal three-dimensional but planar fibre networks

The three-dimensional structure of paper can be simulated with a sedimentation-like or growth process. This allows a systematic study of the stochastic fibre network structure of paper as we will explain next. The approach has a number of limitations that we will discuss after that.

A moment's consideration makes it clear that with increasing grammage—from the 2D limit—pores start to appear due to stiffness of fibres. Fibre stiffness prevents them from bending so much that they would always touch their nearest neighbours in the thickness direction. The sedimentation model of paper assumes that the sheet is formed from a dilute suspension under the influence of a uniform flow field. All fibre interactions are ignored. The resulting porous structure is hyperbolic: instead of pore sizes it is characterized by the distribution of free spans between fibres in the in-plane and out-of-plane directions [78–80]. The formation of the structure leads directly to the question of how to measure and characterize a pore system so as to relate it to transport properties [81].

The network structure of the sedimentation growth model is controlled by three parameters: fibre thickness, fibre width and a measure of the uniform drag force over fibre stiffness. The first two parameters simply define the length scale for the free-span distributions in the in-plane and out-of-plane directions, respectively. The third parameter controls the porosity of the network. One possibility is to define the maximum deflection in the out-of-plane direction T_f [61]. If a fibre would need to 'bend' more than this to make contact with the network below, an open space would be formed instead (an example is shown in figure 14).

At low basis weights (remember this is what the mass per unit area of paper is routinely called) on a flat substrate, there are no open spaces in the thickness direction. As the basis weight grows, the roughness of the top surface of the network grows. At some point fibres can no longer adjust to this surface roughness because their stiffness is too high compared with the drag field. After this point, free spaces (or 'pores') start to form between the fibres in the thickness direction, and soon a homogeneous 3D bulk phase grows (figure 15) [79].

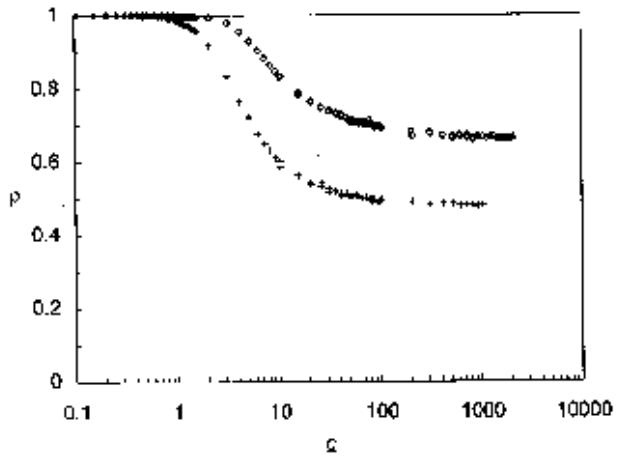

FIG. 2. Density ρ against coverage $\bar{c}$. $F=1$ (+) and 2 (◇), fiber length $l_f=21$. Two system sizes, $L=1000$ and 100 (the latter at high coverages).

Figure 15. Cross-over from two-dimensional to three-dimensional sheet structure when basis weight increases. For stiff fibres the transition occurs at lower basis weights than for flexible fibres. This happens because stiff fibres make the sheet porous, and the pores kill all point-wise fibre–fibre correlations in the thickness direction [79].

Although the sedimentation model is simplistic, it allows one to understand how fibre properties and basis weight influence porosity in paper. At low basis weights, there are at most holes through the sheet. At higher basis weights, the sheet structure can be represented as three layers. Of these three, the two surface layers generally have higher density than the interior bulk layer. If fibres are flexible, the surface layers contain a high fraction of the basis weight and little of the sheet structure is left to the bulk layer. The surface of such a network becomes 'rough' and develops interesting fluctuation behaviour [82]. That is, the thickness of the deposit $h(x)$ develops correlations similar to any self-affine profile. This is not due to variations in the number of fibres per unit area (or the basis weight) but arises only from the pore-space structure correlations [82, 83], in analogy with other simplified 'growth models'.

2.4. Real three-dimensional sheet

The sheet structure of real paper differs from the simple random sedimentation model. It depends on all the unit operations of the papermaking process: drainage, wet pressing, drying and calendering [1].

During drainage, the fibre mat is formed either on one wire or in a gap between two wires. The thickness of the fibre mat on the wires grows as the suspension is drained through it. In addition to fibres the suspension contains fines, mineral filler particles and colloidal matter. The retention of the smaller material onto fibre surfaces is controlled by a competition between capture and flushing. The result is a concentration profile through the sheet thickness. In papermaking, the applied pressure over the drainage zone is carefully designed so that small particles are enriched as much as possible on the surface layers of the sheet. This contributes to a smooth surface that is covered with uniformly distributed small ($\mathcal{O}(1\mu\text{m})$) pores, an ideal case for good print quality.

[1] See also the other books in the series of [1].

Typical solids content of the paper web after drainage is 20%. When we take into account that wet fibres contain at least 50% water and dry fibres have an approximate density of $1500\,\mathrm{kg\,m^{-3}}$, we can estimate that if the paper web would be allowed to dry freely after drainage, the resulting sheet would have a porosity close to 80%.

After drainage, the paper web is pressed between felts in a succession of, say, three nips. Typical solids content after pressing is 50%, i.e. half of the water has been removed. At this point some water is already squeezed out of fibres, both from the fibre lumen (the open space inside each fibre) and from the gel matter of the fibre wall [84].

In the pressing of the wet web the total pressure on fibre surfaces consists of hydrodynamic and structural pressure in parallel [85]. The compression of the sheet structure in wet pressing is inhomogeneous. Local areas of high basis weight experience higher structural pressure from the nip than areas of low basis weight. Along individual fibres, the compressive structural pressure is mediated by inter-fibre contact areas. Free spans between contacts experience only the drag force but little compression. After the pressure nips the sheet structure recoils and expands depending on the type of fibres used. The recoil is also inhomogeneous.

The pressing of the wet fibre network bears some analogy with the compression of granular materials. The contact interaction between individual grains corresponds to the stress transfer at inter-fibre contacts in paper. However, the lateral stresses are different. Because of the high flexibility of wet fibres and the large fraction of fibre surfaces in contact with others it seems that sheet compression creates little transverse shear forces [86]. It is probable, though certainly not proved, that compressive forces are transmitted almost entirely in the thickness direction. This is an analogous situation to the so-called q-model of stress transfer in granular packings [87]; in the case of paper or fibre networks similar toy-models and experiments seem to be missing. In the drying water evaporates out of fibres. This makes the fibres shrink. Shrinkage occurs predominantly in the transverse directions of each fibre. The reason for this is the helical fibre wall structure where partly crystalline cellulose microfibrils spiral around the fibre axis. Water uptake and hence swelling happens in the hemicellulose matrix between the microfibrils. The cross-sectional area of fibres decreases by 20–40% upon drying. As a result, sheet thickness and porosity decrease. The free span distribution changes, but because of the inhomogeneity created in wet pressing, the change can be non-monotonic.

The fine particles deposited on fibre surfaces during drainage influence the shrinkage of the structure during drying. Fibre fragments rich in hydrophilic microfibrils can build bridges between fibre surfaces and pull them into contact during drying. This can be seen as a reduction in porosity and mean free span lengths. Microfibrils stretching out of fibre surfaces have the same qualitative effect. Fibre fragments rich in hydrophobic lignin, as well as mineral fillers, act in the opposite directions, contributing to higher porosity in dry paper (figure 16 illustrates the effect).

Calendering is the last phase in ordinary papermaking to 'iron out' some of the surface roughness. In calendering the paper web is run through a set of hot cylinder nips of high pressure. Moisture (steam) is applied on the surfaces of the dry paper web. Since the radius of calendering rolls ($\mathcal{O}(1m)$) is much larger than paper thickness ($\mathcal{O}(10^{-4}m)$), the nip contact is very flat and therefore the Hertz problem is not applicable. Calendering acts to flatten the highest peaks of the thickness distribution [89,90]. An example of two real papers, calendered and non-calendered, is provided in figure 17.

This is a bit surprising because one might expect that local point-like compression would be mediated along fibres also to the surroundings. The thickness and the basis weight are certainly related to each other (figure 18 shows some typical data). As one might expect, after calendering there is a correlation between local density and local basis weight (figure 19 illustrates the scale thereof) [91].

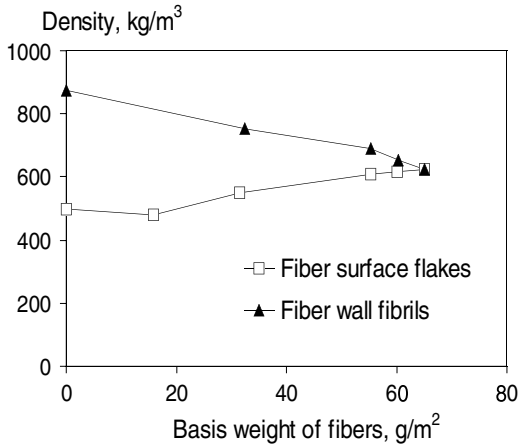

Figure 16. The effect of different fibre fragment additions on sheet density, when their fraction is changed and the total basis weight is kept constant [88]. The fine particles arise naturally in the process of extracting the fibres from wood.

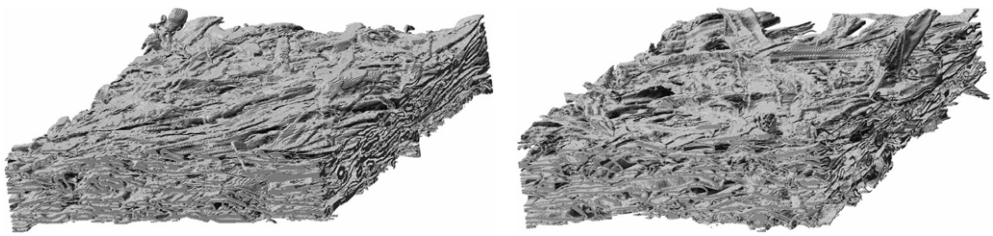

Figure 17. Two different examples of 3D newsprint structure measured by x-ray tomography (courtesy of Oyvind Gregersen, NTNU, Norway). The left panel shows a calendered structure while the right panel case is uncalendered.

Considering all the mechanisms of fibre interaction in the above unit operations, it is rather surprising that experimental data on the free span distributions in real paper agree fairly well with the assumption of a completely random uncorrelated structure that we discussed previously. Even the quantitative agreement is reasonably good for the z-directional free spans. For the in-plane directions the free-spans do not agree with the expectations—the distribution is not quite exponential—presumably because sheet compression causes fibres to twist around their axes [92]. Since fibres are relatively flat ribbons (cross-sectional aspect ratio = 5–10 cf table 1), twisting reduces significantly the effective mean cross-section of fibres in the in-plane directions but only a little in the thickness direction. The short span repulsion observed in the ideal sedimentation model is clear also in real paper data.

There are two 'classical' ways of measuring the pore-related properties of paper [93]. One is the mercury porosimetry used to characterize the pore spaces of various media in general. Paper might be somewhat complicated in this respect due to the fact that its structure is relatively soft. Then, the detailed nature of the pore-space—local correlations between the neighbouring pores sizes, etc—can be important. Usually a mercury intrusion experiment is interpreted by assuming that all voids up to a certain effective hydraulic radius are filled. This can be obscured by local 'flow out of bottle' effects for instance: interconnected pores make the interpretation of the intrusion process less trivial since a small pore can hinder the access to or from a large one (as in ketchup bottle) [94]. Another indirect characterization is time-of-flight

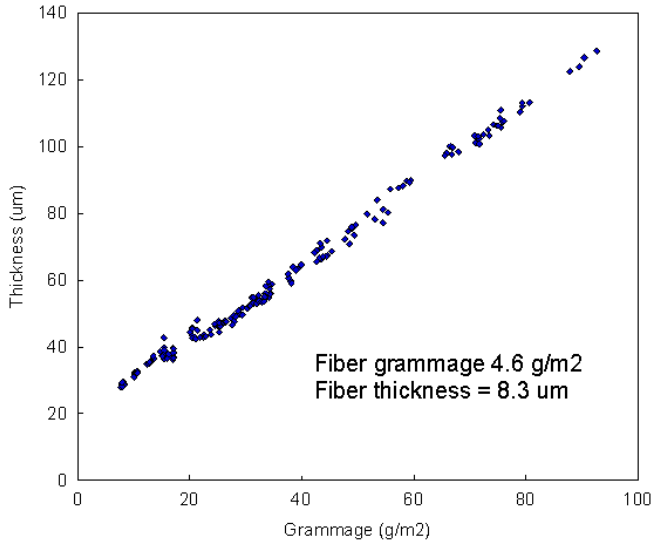

Figure 18. An example of sheet thickness versus the basis weight (grammage).

laser spectroscopy, in which the delay of a sharply defined laserpulse is monitored. The evidence provided by this method suggests strongly that the scattering surfaces inside paper give rise to a typical mean free path for photons of about two micrometres, i.e. much smaller than the typical pore size [25]. Then, one can reconstruct the pore and solid phases from x-ray tomographic images. In the case of paper, this is hampered by the still not quite sufficient voxel sizes ($\mathcal{O}(1\ \mu\mathrm{m})$ typically at best): this means that the imaging is not able to depict the smallest pores, and there are interpretation problems. Nevertheless the results are encouraging [95–98], and in this review we use such results.

The topology of paper surfaces has been studied little. Usually one just measures the rms deviation of surface height. A lot about fibre deformations and interactions could be learned from the analysis of surface textures. The rough sheet surfaces can account for as much as 10% of the total thickness. One reason for the limited interest in the surface topography has no doubt been the slow measurement techniques [99]. The softness of paper surface limits the use of mechanical profilometry. Interferometric imaging techniques have only recently become available. When combined with detailed models of the network compression, they promise ample opportunities to improve the situation [100].

3. Paper as a solid—elasticity, viscoelasticity and fracture

3.1. Mechanical properties of papermaking fibres

In the first approximation, papermaking fibres are elastic–plastic beams. In the paper sheet, there are 10–40 inter-fibre bonds per fibre. Because of the high coordination number, the in-plane mechanical properties of paper are similar to the axial mechanical properties of fibres.

The morphology of wood fibres consists of several layers of different structures. The thickest of these, the S2 layer, has a helical or chiral structure made of microfibrils. The microfibrils are bundles of crystalline cellulose, connected together through segments of amorphous cellulose. Thus there is a strong similarity to other biologically originated materials with a fibrous or fibril geometry, like bone, in that a fibre is a two-phase composite.

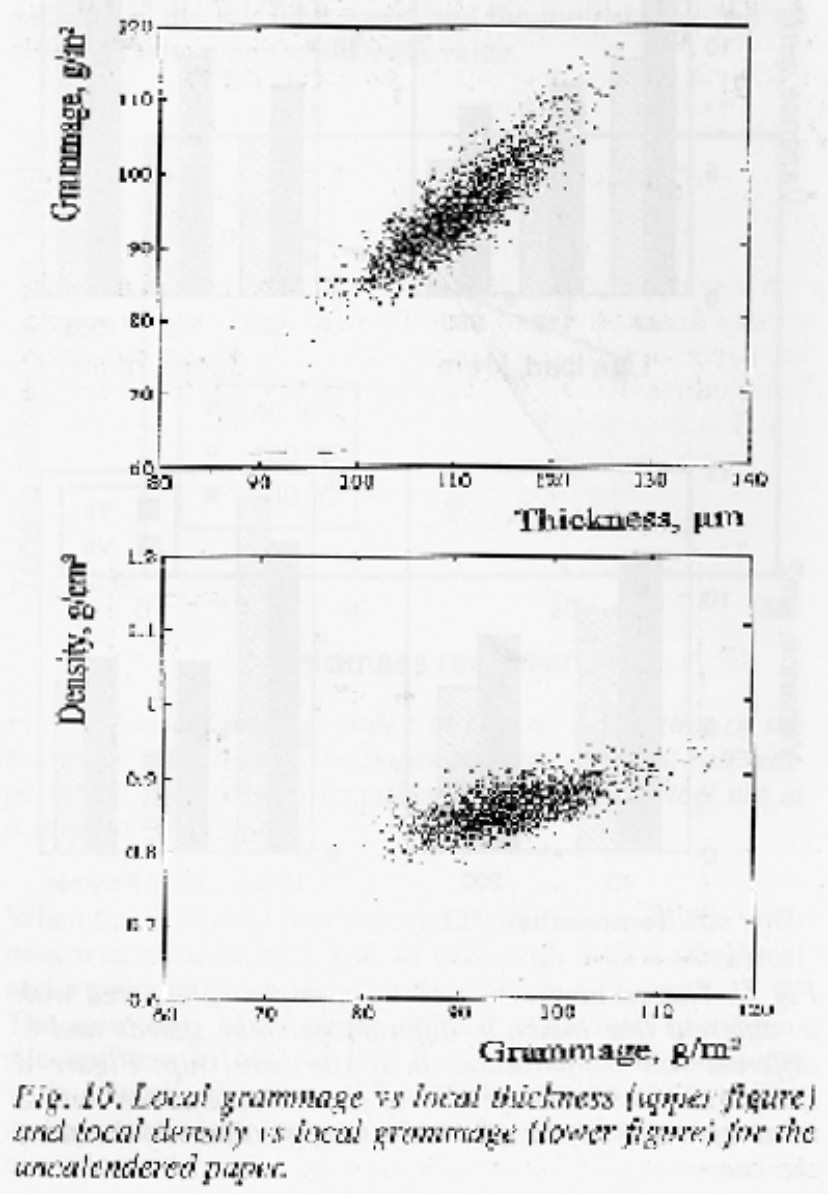

Figure 19. Point-wise correlations between local basis weight and local density. The figure demonstrates that there are correlations, which stem from the response of the local structure to, for example, wet-pressing [91].

The cellulose microfibrils are, for all practical purposes, ideally elastic up to the point of failure. When the fibre is strained in the direction of its axis, the observed elastic modulus can be simply estimated from the elastic modulus of cellulose, 25 GPa, modulated by the chiral angle of the microfibrillar helix. This microfibril angle displays a lot of natural variability but the mean value is usually less than 10° off the fibre axis. Hence the elastic modulus of a fibre is close to the elastic modulus of cellulose [35, 101]. The chirality of the fibres of almost all

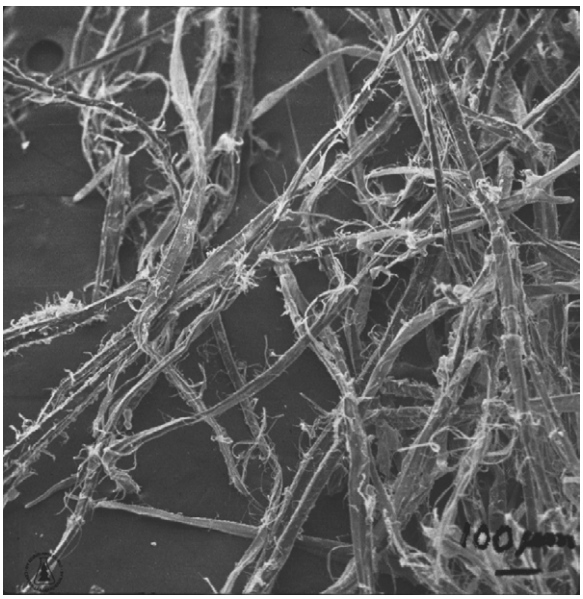

Figure 20. Wood fibres photographed. From [1].

wood species is always right-handed. This microscopic asymmetry leads to some interesting macroscopic effects (twisting under tension, chiral curl (as mentioned in the introduction)) [53].

Depending on the pulping process, various amorphous hemicelluloses and lignin may be present between the microfibrils. Hemicelluloses soften easily in humid or hot climatic conditions and have a much lower elastic modulus than cellulose even in the room conditions. Thus the elastic modulus of a papermaking fibre can be smaller than the elastic modulus of cellulose.

The outmost layers of wood fibres hold the fibres together in the wood material. These layers are removed, in part or completely, when the fibres are disintegrated in a pulping process. The remaining fibre structure may also suffer mechanical damage. The induced damage and natural imperfections of the fibre often act as weak points for fracture. See figure 20 for a schematic picture of fibres.

Structural imperfections are induced into the fibres also in the papermaking process. Suspension flow and drainage on the wire create curl, twist, dislocations and pressing 'undulations' in the thickness direction of the sheet. Fibres have to bend up and down to accommodate each other as was earlier noted related to the 3D structure. Drying fibres shrink primarily in their lateral directions (in wet fibres there is water between the microfibrils, not inside the microfibrils). (Since the microfibrillar angle is small, fibre thickness decreases much more than fibre length.) Shrinking water menisci between the fibres pull fibres together. This process creates various deformations in the fibres, such as dislocations and compression zones at the fibre crossings [102, 103].

3.2. Fibres' influence on paper mechanics

The mechanical properties of paper can be varied significantly by selecting different types of fibres and fibre fragments in the sheet. The variability is illustrated in figure 21.

The fibres in paper are full of imperfections and exhibit a wide variety, of natural origin, in dimensions and mechanical properties. The elastic modulus, plastic elongation and creep of

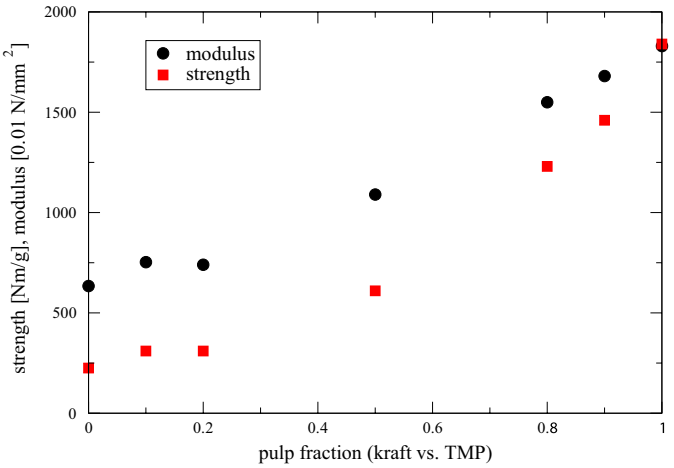

Figure 21. The tensile strength and elastic modulus of binary mixtures of two fibre types. (Courtesy of J Sirviö, KCL.) Notice the more non-linear behaviour of the strength with the mixing ratio.

paper are all dependent on fibre properties. Fibre properties follow from the type of pulp used. They can also be modified by the mechanical treatment, or beating, of the pulp. Beating is a standard operation in papermaking. Its purpose is to increase the flexibility of the wet fibres which results in higher density and higher inter-fibre bonding.

The elastic modulus of paper is smaller than the elastic modulus of the fibres because of the porosity of paper (pores carry no load) and the random orientation of the fibres in paper (all fibres do not carry full load). In addition to these effects, the elastic modulus of paper is in practice very much dependent on the elastic properties of the fibres in paper [104].

Inelastic elongation of paper arises from plastic elongations that take place in the fibres. Fibres elongate plastically when microfibrils slide relative to each other, either at the isolated structural imperfections or fairly uniformly all along the fibre length. The first mechanism is more common than the second. The inelastic behaviour of paper is controlled by the mechanical properties of the fibres that the paper consists of [105].

The rate-dependence of the load-elongation behaviour, the stress relaxation and the creep phenomena characterize the rheological behaviour of paper. Paper is a viscoelastic, plastic material. In that respect, it is quite similar to many polymers. The softening of the amorphous components of the fibre wall, hemicelluloses and lignin, controls the viscoelastic properties of paper. Moisture strongly influences the softening making it appropriate to consider moisture effects in connection with rheology. The rate of loading especially controls the stress–strain state of wet paper.

Paper is not simply a linear viscoelastic material. Its stress-strain behaviour cannot be explained by viscoelastic changes in the elastic modulus. Instead, the nonlinear part of the stress-strain curve corresponds to an irreversible elongation—a truly plastic response. Paper can therefore be properly characterized as a viscoelastic, plastic material [106, 107].

Fibre failures do not explain the inelastic elongation of paper. Even when paper fails, few or by far not all of the fibres that cross the crack path fail. An example of this fact is visible in the figure 5 shown in the introduction. Only if the inter-fibre bonding is exceptionally high (very dense structure such as with grease-proof paper), the majority of the fibres across the macroscopic failure line break. Even in this case the fibre failures take place just before the macroscopic failure point, well after the inelastic behaviour of paper has begun. This naturally

means that paper is not exactly 'quasi-brittle', like for example concrete, in this respect since in a tensile test the stress-strain curve $\sigma(\epsilon)$ derives its shape from the plastic deformation and not from a decrease in the elastic modulus due to damage, only. In passing this gives a practical way of measuring the irreversible strain, by assuming that the total strain is composed of reversible and irreversible components ($\epsilon_{\rm pl}$) and that the elastic modulus changes very little: $\epsilon_{\rm pl} = \epsilon - \sigma\epsilon/E$.

In the majority of paper grades, macroscopic failure occurs when bonds between the fibres on the crack path break. Paper fracture is therefore a fibre network process. It is not governed by the fracture properties of individual fibres. The inter-fibre bonding is controlled by paper density, or the RBA.

The bonds between fibres are physically just a 'boundary condition'. However, technologically they constitute another 'phase' because one can alter inter-fibre bonding much more easily than fibre properties. For example, pulp beating improves also inter-fibre bonding. One can also add starch or other bonding polymers to paper. Fibre surfaces are rough on the nanometre scale. Bonding polymers of high molecular mass are needed to bind fibre surfaces together.

The degree of inter-fibre bonding can be characterized with z-directional strength measurements of paper. In these tests, double-sided adhesive tape is usually used to transfer tensile stress to the thickness direction of paper. Typical values for the z-directional tensile strength are a few hundred kilopascals [108].

3.3. Elasticity of paper

A two-dimensional fibre network is a pertinent approximation for the load-bearing geometry (figure 22). This is again especially so at low basis weights because fibres are up to 100 times longer than the paper sheet is thick. Tensile stress applied to a paper sheet is transmitted predominantly parallel to the sheet plane, as axial stresses in fibres.

In an ideal two-dimensional network of long straight fibres, the elastic modulus depends on the flexural stiffness of the fibres and the shear stiffness of the inter-fibre bonds. If both of these stiffnesses were low compared with the axial Young's modulus, a spring network would be the appropriate theoretical analogue. In the case of real paper, the shear stiffness of the inter-fibre bonds is relatively high. The distance between inter-fibre bonds is of the same order of magnitude as the width of the fibres. Under these circumstances, paper is best approximated as a two-dimensional random beam network.

In a two-dimensional network the ordinary bulk density, ρ, is replaced with a line density, q, or the total fibre length per unit area. Since a two-dimensional network has no thickness, the ordinary elastic modulus (= force per cross-sectional area divided by strain) cannot be defined. Instead one can use the elastic modulus, i.e. divide the applied force per unit width of the specimen with strain and basis weight (the latter to normalize with respect to mass).

Figure 23 shows elastic moduli from a set of paper sheets of different basis weights or different line densities, q. One can see that in this case the elastic modulus approaches zero at the basis weight of 5 g m^{-2} or so. At the other end of the scale, the elastic modulus becomes constant above ca 45 g m^{-2}.

When the two-dimensional line density is well above the percolation threshold, only the free ends of the fibres reduce the elastic modulus of a two-dimensional beam network. The free ends do not carry any load. If one considers the elastic energy of a strained fibre network, it is easy to see that the elastic modulus should be proportional to the total fibre length that carries the full load. In fact the elastic modulus is somewhat smaller because the stress level in a fibre cannot jump from zero at the free end segment to the full level in the first loaded

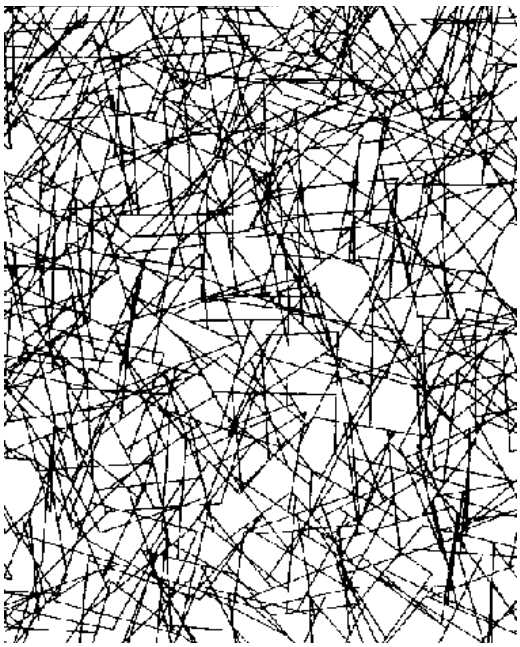

Figure 22. An example of a 2D 'simulation network'. Here, the dead ends of fibres have been removed so that only the load-bearing part of the structure remains.

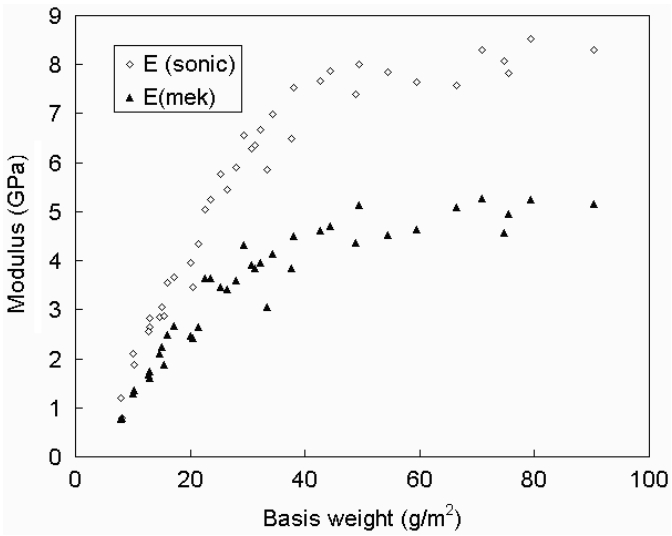

Figure 23. Elastic modulus against basis weight, measured ultrasonically and mechanically [109].

segment. Some of the segments close to fibre ends are only partially loaded. This is described by the often-used Cox theory of the elasticity of a fibre embedded in a matrix, with shear stress transfer. This predicts that the stress state of a fibre is given by a tanh-shape function along it and a (trivial) angular dependence with respect to the external stress, so that for the strain along the fibre one has $\epsilon_f = \epsilon_s(1 - (\cosh kx/(\cosh kl_f/2)))$ [110–112]. Here k measures

the stress-transfer from the matrix (crossing fibres in paper) due to shear. In other words, the stress changes gradually such that the whole fibre's elastic energy is dependent on the shear stress transfer and on the length l_f as well, in particular.

Now it is easy to see that the mean length of the free ends of a typical fibre should be proportional to the typical distance between two nearest-neighbour inter-fibre bonds, or $l_s = 2/\pi q$ [62]. Thus elastic modulus should be proportional to $E \simeq q * (1 - \lambda l_s/l_f)$ where $\lambda > 1$ depends on the rate at which stress increases from zero to maximum at the fibre ends. Given that $l_f \simeq 5.7/q_c$,

$$l_s/l_f = 2q_c/(\pi * 5.7 * q) = 0.1q_c/q. \tag{1}$$

Two-dimensional random fibre network simulations have verified such behaviour, qualitatively [112–115]. The major disagreements concern the precise value of the prefactor in $E \sim aq$ and the value of the constant λ. They also reveal that for q not much larger than q_c fluctuations are important if one considers the stress-state of any individual fibre, in contrast to the Cox-theory [112].

Such stress fluctuations should, of course, get reduced with q increasing, but then one runs into the fact—for paper—that the three-dimensional structure takes over. All this basically can be translated to read that as in other models of elasticity of disordered media, the elastic modulus in the percolation-limit (i.e. its dependence on $q - q_c$) can be understood via 'scaling' concepts, but more quantitative measures are sometimes difficult to compute. Indeed, while the elasticity or even fracture of fibre-reinforced composites is in many cases well under control [116], there is not yet any comprehensive theory of fibre networks which would work quantitatively. One needs to understand the relative roles of axial and shear deformations—even in a simplified scenario where the network is decomposed into segments, with deformation energy, and bonds where the segments meet—plus the contribution of disorder in terms of varying segment lengths. This last effect means that a typical segment responds to the external deformation according to its shape as long, narrow ones have a smaller resistance to bending.

There is also a geometric explanation why inter-fibre bonding has relatively little influence on the elastic modulus of paper. Since the free segment length is similar to fibre width there are, e.g. 50 inter-fibre bonds per fibre. This means that the free fibre ends correspond to a few per cent of the fibre length. Even if the connectivity changes by a factor of two, the active fibre length would always be over 90% of fibre length, i.e. essentially constant [104].

Lastly, one should also incorporate the fact that fibres are fibres, and there are collaborative effects taking place: segment stresses along fibres are correlated. In the context of network reinforcement (discussed below in more detail) this is considered in figure 24: a mixture of two kinds of fibres does not follow a linear-rule-of-mixtures, so that for a basis weight fraction $0 \geqslant f1$ one would have $E = fE_2 + (1 - f)E_1$ where E_i are the moduli of the different kinds of fibres (see also figure 21). However, if the network is constructed instead such that fibre segments are assigned either of the two elastic moduli randomly, this will turn out to work well. The effect of disorder, in general, can of course be analysed more theoretically by averaging over a locally varying 'elastic modulus field' $E(x)$ [117]. The problem and advantage of such an approach lie in that one essentially linearizes the dependence of the averaged $\langle E \rangle$ on the strength of the variation. The conclusion is then that there are local correlations with strain and elastic modulus $E(x)$ and that the averaged quantity - E - decreases with the introduction of local variation [118].

In the 3D limit, an analogue is an ideal homogeneous porous solid, whose elastic modulus would be linearly related to porosity or density ($E = E_0\rho$), at least when porosity is small. At large porosities structural deformations appear, initiating a faster reduction in the elastic modulus. Nevertheless, the linear density dependence of elastic modulus should be observed

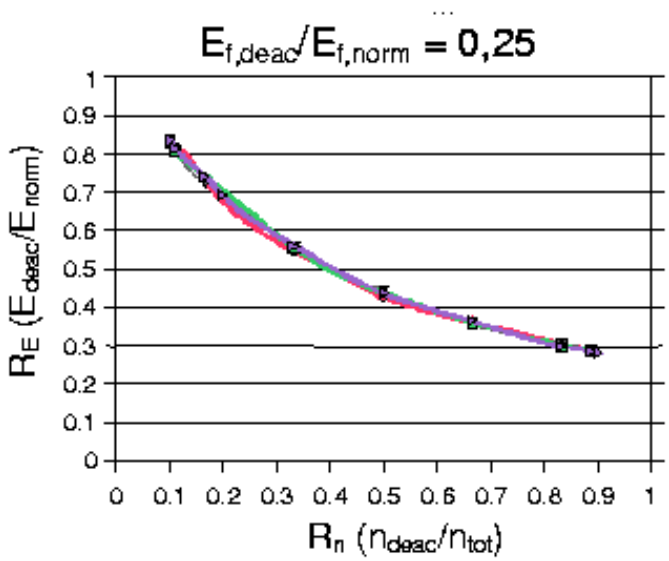

Figure 24. The elastic modulus of a 2D fibre network: here the fraction of fibres is varied so that the 'less stiff' ones have an elastic modulus of 1/4 of the stiffer ones. Clearly, the behaviour as a function of the mixing ratio is non-linear, thus a linear rule-of-mixtures does not work, and in fact a 'segment' on a fibre has a stress-state correlated with the neighbouring ones on the same fibre. Courtesy of T Rinne.

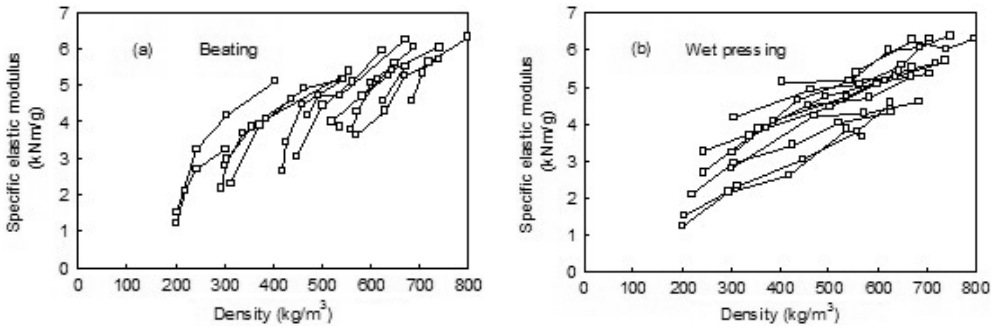

Figure 25. Elastic modulus of paper against density. Density was increased both by pressing the sheet more and by more mechanical beating of fibres. See [104].

when small strain levels are used. One can see from figure 25 that paper does not behave as an ideal homogeneous porous solid would, since one can see much variation of E at a given density. The two methods of changing density, beating and pressing, give paper different elastic moduli when compared at equal density. This demonstrates that density alone or network structure alone does not define the mechanical properties of paper. As discussed in section 2, the structure of paper is very close to a fully random, uncorrelated planar fibre network. This means that the connectivity of the fibre network, the number of inter-fibre bonds per fibre, is controlled by the density or porosity of paper. The source of the differences seen in figure 25 must lie in fibre properties.

The factor that dominates the elastic modulus of paper is the effect of drying stresses, which has a much larger effect than bonding degree [119]. The same can also be demonstrated by

computer simulations [120]. It has been shown experimentally that the mechanical properties of a fibre depend on the axial stress applied on the fibre during drying [121]. If the fibre is free, its elastic modulus becomes much smaller than it would if the fibre is strained. The analogous mechanism applies to the fibres in a paper sheet. If paper is dried under tension, the elastic modulus of fibres is larger than if the paper is free during drying. The influence of the drying stress can also be seen in the flatness of the sheet. Freely dried paper sheet is wavy and cockled, 'slack' in appearance. The same difference between slack fibre segments and taut fibre segments characterizes the structure of freely dried and restrained dried paper (see figure 1 again) [121]. In ideal situations paper is dried in such a manner that shrinkage during drying is prevented. On a paper machine this can be accomplished by maintaining a tension on the paper web in the 'machine direction', the direction in which the paper web runs through the machine. In the lateral 'cross-machine direction', no stress can be applied at the edges of the web. Therefore the lateral shrinkage is practically free at the edges of the web. In the middle of the web, most of the shrinkage is prevented by in-plane shear forces [122].

Beating is a mechanical treatment of the fibres that opens up their helical fibril structure. The swollen fibre walls are conformable and flexible, which promotes inter-fibre bonding. Second, the opening or swelling of the fibre wall structure means that the fibres will shrink during drying when water is removed from the fibre wall. The swelling degree increases with beating, and if shrinkage is prevented, drying stress also increases with beating.

In other words, the elastic properties of paper are in practice primarily controlled by the elastic properties of fibres, not by the fibre network structure. It has indeed been demonstrated that at high densities, the elastic properties of paper are equal to those of a laminate that is composed of fibre wall layers. On the other hand, the mechanical properties of fibres are very sensitive to the network structure. fibre curl, kinks, etc can have a detrimental effect on the elastic modulus of paper if drying is free or if the network structure has a high porosity that leaves long fibre segments free.

Adding water softens paper. This is only very natural since the cohesion of paper forms in the opposite process of drying. At the molecular level water disrupts hydrogen bonds of cellulose and other polysaccharides of wood fibres. Thus not only do the bonds between fibres become weaker as moisture content increases but also the matrix between cellulosic crystals softens. The cellulosic crystals or microfibrils do not soften with water addition.

The thermodynamic effect of water on hydrogen bonds explains reasonably well how the elastic modulus of paper decreases with small amounts of added water. The analysis of Nissan *et al* [123] predicts that elastic modulus $E \sim \exp(-C_I \times m_c)$, where C_I is a 'co-operative index' and m_c the moisture content. The values of C_I seem to depend on the level of drying stress at which paper was dried, the very same factor that controls the elastic modulus in dry paper. At high drying stresses, C_I is smaller than at low drying stresses [124]. A plausible interpretation is that even the molecular level alignment of cellulosic microfibrils increases if the drying stress is increased. The macroscopic rectification of fibres especially in the bonded segments is clear from microscopic images. These structural changes lead to higher elastic modulus because the microfibrils carry proportionately more stress than the low-modulus matrix between them. The corresponding influence on the moisture sensitivity of the elastic modulus of paper is obvious because only the matrix softens with moisture addition. The corresponding dependence on drying stress is also seen in the hygroexpansivity of paper.

At high moisture contents, the elastic modulus decreases much more rapidly than predicted by the hydrogen bond effect. In wet conditions fibres slide past one another [125]. This means

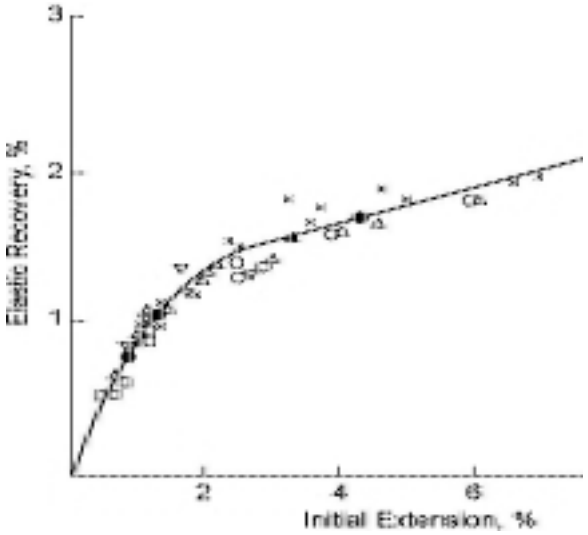

Figure 26. Elastic recovery of strain as a function of initial extension [128]

that the elastic modulus of paper is controlled mostly by the viscosity of the water menisci that couple fibres together.

3.4. Visco-elasticity and plasticity

The dependence of the stress–strain curve on the strain rate shows the viscoelastic nature of paper [126, 127]. At fast strain rates the measured stress is higher than at slow strain rates. This simply implies that more time is available for stress relaxation during the test. The elastic modulus and tensile strength of paper increase with the strain rate, but the breaking strain may increase, decrease or remain constant. Recent experiments suggest that the breaking strain is independent of the test dynamics at least under compression. Paper is generally stiff and brittle at high strain rates and soft and ductile at low strain rates [38, 126, 127].

One of the interesting rheological properties of paper is delayed recovery. Following a stress–strain cycle, the remaining strain at zero stress is ordinarily described as the 'permanent' or the plastic strain. In fact, this strain component is time-dependent. In other words, after a strain-release cycle most of the recovery of paper takes place at around 10 s [126, 128].

The amount of delayed recovery increases with the initial elongation to which paper was taken before returning it to zero stress. This is true even at initial elongations that are in the linear region of the load-elongation curve below the yield point. In the experiments displayed in figure 26, the delayed recovery was measured 24 h after the initial elongation. The elastic recovery was determined immediately after the specimen had returned to zero stress. Plastic, truly permanent, elongation does not occur below the yield point.

Another characteristic of the visco-elastic–plastic nature of paper is ageing [129]. In ageing, time-dependent changes in humidity, temperature or applied stress cause a change in the mechanical properties that recovers slowly. Again, in paper this is similar to other polymeric materials and couples the elastic properties to the molecular level. The concept of molecular free volume often explains the recovery process. For example, straining leaves paper in a thermodynamic non-equilibrium state where the molecular level free volume in the fibre wall is large. The initial relaxation process is fast because there is room for intermediate configurations

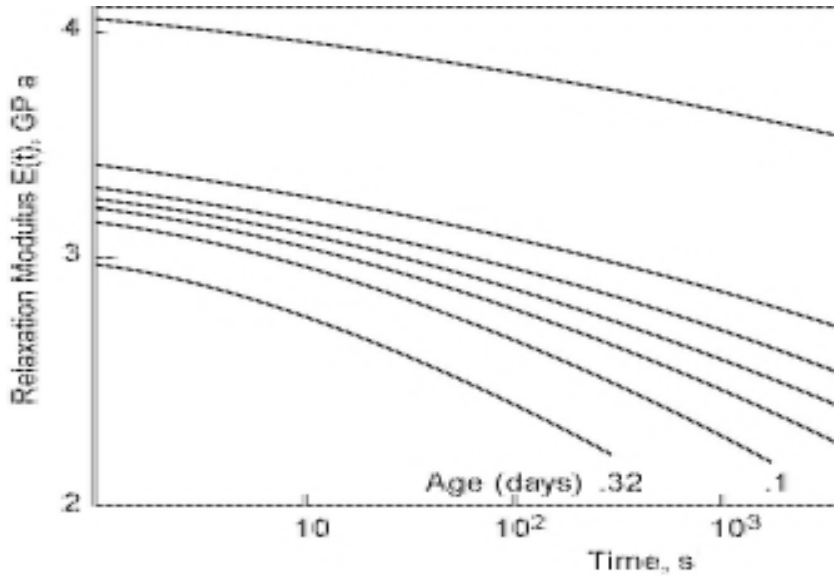

Figure 27. Stress relaxation after different ageing times (logarithmic scale) counted from a de-ageing treatment. Relaxation is expressed by the relaxation modulus that is the ratio of the decaying stress and constant strain [129].

through which the relaxation process must proceed. The approach to equilibrium corresponds to a decay of the free volume and to a slower relaxation rate. This mechanism has been demonstrated in polymeric materials [130] (see figure 27).

The plastic elongation of paper generally causes little change ($<10\%$) in elastic modulus at sub-fracture strain levels as noted earlier. After some elongation-recovery cycles, the stress-strain curve of paper exhibits more and more linear elasticity. If we elongate a paper sample almost to failure and then release, the resulting sample is almost perfectly linearly elastic all the way to failure. Thus there is a maximum level of 'intra-fibre' irreversible deformation as one could expect.

Plastic elongation creates localized damage to paper. If elongation is further increased, one of these local damage sites would then trigger the failure of the paper sample, i.e. it is plausible that the 'sites' created during plastic elongation act as defects which have the potential of causing the macroscopic failure of paper. The sizes of such sites in a plastically elongated paper have not, to our knowledge, been studied in detail. This line of reasoning is in fact quite similar to the 'shear transformation zone' theory of plastic deformation in amorphous solids [131]. This addresses the localization in terms of populations of similar kinds of local deformation 'sites'. In terms of orders of magnitude, the sites' sizes should be of the order of fibre length, the scale on which elastic deformations become roughly uniform. Such localizations can be seen in figure 28, and their dynamics and geometry would merit further study [132].

Barkas explained long ago the hysteresis in paper moisture content mentioned in the introduction through swelling stresses. These cause irreversible plastic deformations, and they are created in the fibre wall since crystalline cellulose does not swell. At small amounts of absorbed water the deformations are elastic, but with increasing amounts of water the stress may exceed a yield limit and cause plastic deformations via, e.g., the slip of weakly bonded micelles, freeing more OH-groups to absorb water [56].

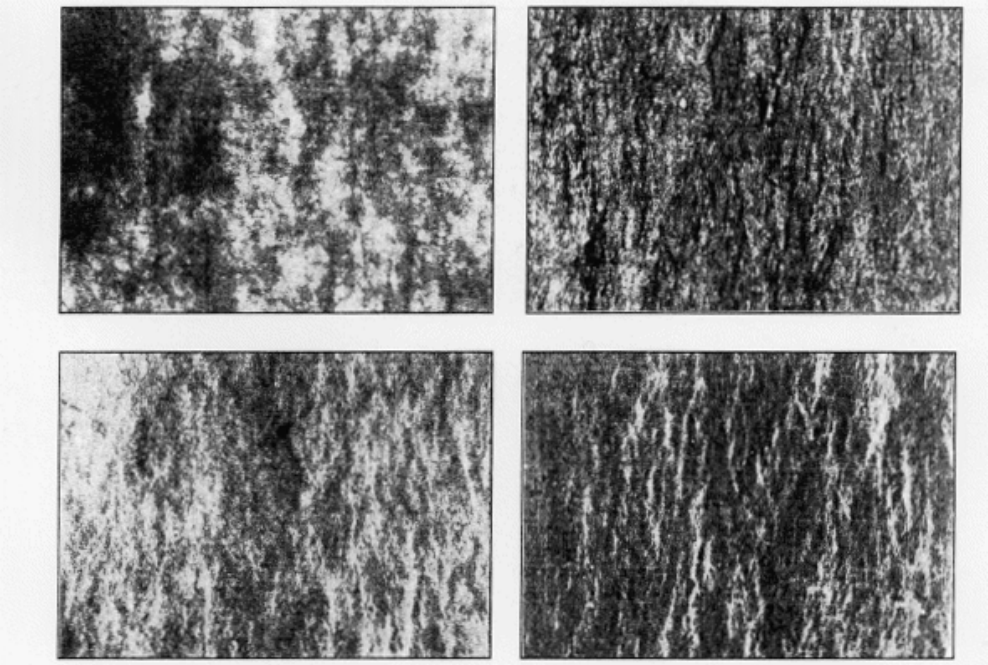

1. Photographs of strained CD paper strips; back-lit linerboard (A) and newsprint (B) at a high magnification (100X), and the same specimens front lit (C and D). Direction of straining is horizontal.

Figure 28. Distribution of local plastic strain in paper. Plastic deformation is made visible by impregnation with a silicone that has been cured before the test. The silicone fills all the pores in paper, hence rendering it translucent. Plastic elongation of paper arises from the opening of inter-fibre bonds which creates local light-reflecting surfaces to the areas of large plastic elongation [133].

The creep rate of paper increases rapidly with increasing humidity (figure 29). The increase in creep rate is much stronger than in elastic modulus. For creep to take place, cellulosic microfibrils must slide past one another as rigid bodies. The sliding requires that all the bonds of such a microfibril break. The probability of this is naturally a strong function of moisture content.

The creep rate also becomes high if the external stress, σ, is increased. This effect can be represented with the common master curve formalism, $\epsilon_{\text{creep}}/\sigma = f(\log t + \log t_a) = f(\log(t/t_a))$.

The time scale factor, t_a, decreases exponentially with the external stress. At large times, the master curve function f seems linear (figure 29). Paper creep is logarithmic in that time region. Using usual creep terminology, this is secondary creep, distinguishing the behaviour from the initial primary creep where strain is not linear in logarithmic time and where one in many materials finds the so-called Andrade's law, a power-law scaling of creep rate and strain versus time (typically $\epsilon_{\text{creep}} \sim t^{1/3}$) [134, 135]. At large times, the creep rate again increases when nearing the failure point. This region is tertiary creep [136].

If the paper moisture content is changed very rapidly as in a cyclic experiment, the strains evolve long after the ambient RH has reached a constant level. The rate of strain change after a rapid humidity change is dependent on the direction of the strain (MD or CD) and on the direction of moisture change (see, e.g. [138]). One consequence is accelerated creep since the creep rate is a non-linear function of the moisture content. Thus paper is able to

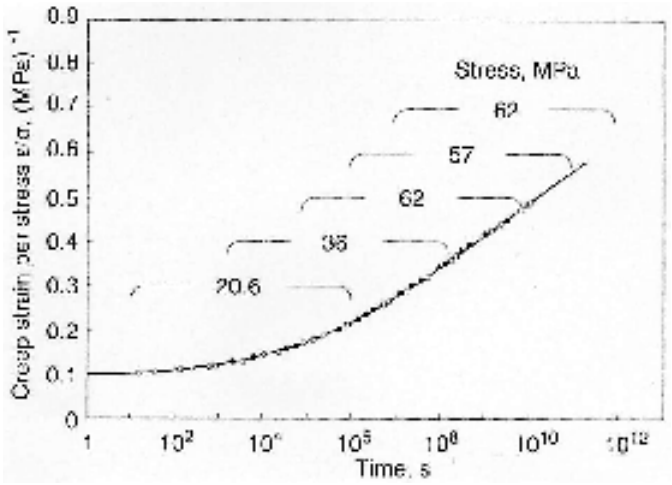

Figure 29. Creep strain of paper at different stress levels, represented through the master curve function f (see text) [137].

creep much faster in a cycled experiment than if the moisture content were kept at the cycle average level.

3.5. Paper fracture

The final failure of paper under tension is a topic with two opposite faces: issues where the disorder present can be forgotten and that where it is absolutely fundamental. On the one hand, it is very clear that inter-fibre bonding is very important for paper strength—if there were no bonds between fibres, paper would have no strength. On the other hand, numerous experiments demonstrate that tensile strength is closely coupled with the elastic modulus of the paper. As a rule of thumb, tensile index is equal to elastic modulus times $1.0 \pm 0.1\%$. There exists no direct measurement for inter-fibre bond strength—indeed it is very tedious to establish a method that would give good representation of the largely different values that inter-fibre bond strength must have in real paper.

Compared with typical linearly elastic materials, the tensile strength of paper shows surprisingly little variability. The most-often used measure, the Weibull modulus α is 15–20 when values 5–10 are typical for, e.g. glass [139]. The homogeneity suggests that the tensile strength of paper is controlled by average features and not by inhomogeneous discontinuous defects or 'weak links', such as holes, dirt specs, shives, etc. Such defects do exist in paper and cause, e.g. web breaks (see figure 30). However, it seems that they are too rare to account for every tensile strength value that one measures in the laboratory. The tensile strength of paper is thus controlled by macroscopic mean properties [133, 140, 141].

The microscopic mechanism that leads to the macroscopic fracture of paper is either a burst of bond failures to release fibres or a burst of fibre failures [142]. Remember that a fibre has typically 50 bonds with other fibres and there are typically ten fibre layers in the thickness direction of paper. Bond failure is the dominant failure mechanism in ordinary paper. In order to release the fibres in a circle of diameter equal to the fibre length, several hundred inter-fibre bonds must break. This leads to large averaging over the distributions of bonding geometries. Even in the case of fibre failure, tens to hundreds of fibres must fail in order to propagate the crack for one fibre length. It is clear that the macroscopic failure of paper cannot be triggered

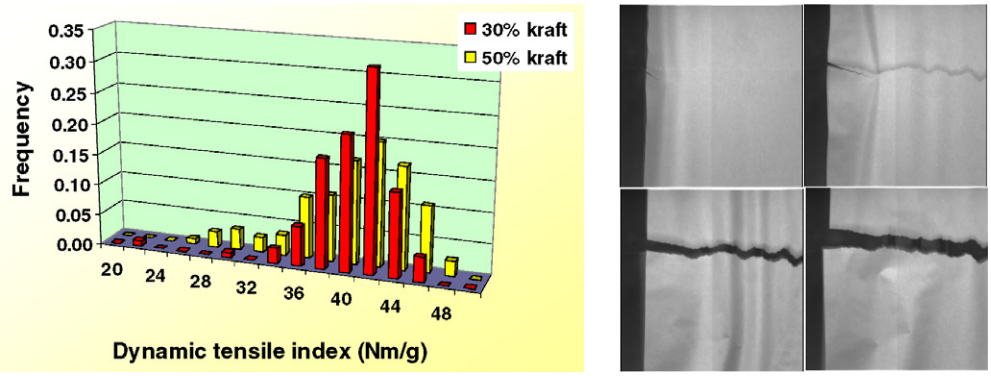

Figure 30. Distribution of breaking stress values of a paper web moving at the speed of 3 m min^{-1}. The main distribution corresponds to laboratory values. Real web breaks occur at much lower stress values where only few breaking stress measurements are made. Clearly the two distributions are separate. In the lower panel, there are examples of crack growth in the same case [140].

by a single microscopic event, and moreover there is residual cohesive strength or in the case of many fibre composites, since the fibres must be 'pulled out'. Bond failure implies that the paper is not extremely brittle in the sense of the usual glass. Necessarily, the damage accumulates over a non-negligible volume compared with fibre dimensions. The same is true for the zone in which plastic work is done around defects, the 'inner plastic zone' as it is called in engineering fracture mechanics.

It has been demonstrated that the in-plane fracture energy, divided by damage width, is closely related to different measures of out-of-plane fracture energy and out-of-plane tensile energy absorption (i.e. Scott bond) [143]. This suggests that there might be a way to use out-of-plane measurements of bonding energy or strength in the calculation of tensile strength [144].

From an engineering viewpoint an important energy-quantity is the fracture toughness or the intrinsic resistance to crack growth. It is *a priori* not clear where the toughness arises from. Paper is not a ductile material in the sense of metals, where dislocations are formed in plastic deformation and whose dynamics is crucial to the understanding of crack resistance. The classical ideas for understanding toughness are similar to those used in composite technology and science. A crack would open up and propagate since fibres are removed by a pull-out from its path. This takes place by opening up the bonds, but energy may also be spent in pure friction [145].

A simultaneous consequence is that the FPZ attains a non-negligible size, and that the quantitative computation of the fracture toughness is not easy. In the former aspect, paper resembles amorphous materials in that the elastic properties average out over a lengthscale that is much larger than the basic, fundamental building block of a fibre segment between two bonds and the FPZ has to be proportional (naturally) to fibre length. There are no studies of the self-averaging and its relation to plasticity (as for amorphous glasses, e.g.) [146, 147].

One question that may then be asked is what is a right measure for the 'disorder' in paper? A good parallel for this is the Dugdale–Irwin approach to the strength of ductile materials. One writes for its scaling as a function of defect size a

$$\sigma_c(a) \sim 1/\sqrt{(a + a_{\mathrm{pl}})}, \tag{2}$$

where a_{pl} measures the size of the inner plastic zone. One may now try to define a similar measure 'w_d' for the effect of intrinsic disorder or, likewise, the scale on which damage accumulation will take place in crack propagation and postulate that for paper one may assume

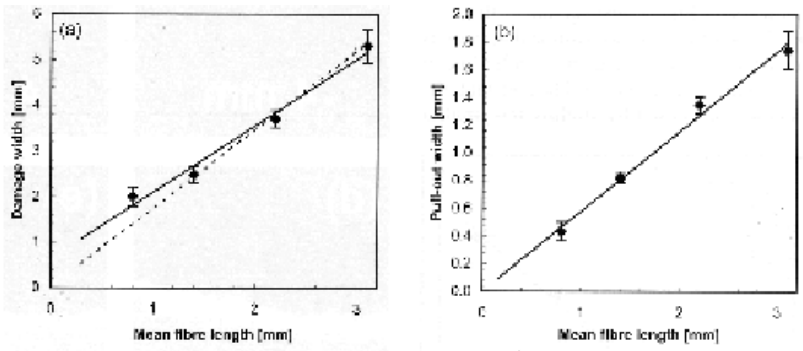

Fig. 2. Damage width (a) and pull-out width (b) of the fibre length samples against the length-weighted mean fibre length. The error bars show the 95% confidence interval. The straight lines (solid and dashed) are drawn for illustration.

Figure 31. Width of the fracture process zone (w_d) against the mean fibre length [148].

$\sigma_c \sim 1/\sqrt{(a + w_d)}$. An implication then is that the strength without any external defects is found by setting $a = 0$. Such a damage width can be measured in practice by optical means, using the changed transparence of paper (see figure 5) [148].

Indeed, one can also demonstrate that if damage width is used in linear elastic fracture mechanics as the critical defect size a as above, reasonable agreement results between the theoretical prediction and the experimental measurement of the tensile strength of paper. Naturally one can also demonstrate disagreements between the linear elastic fracture mechanics and actual measurements of the tensile strength of paper so the theory is not perfect. However, it is not clear whether some of the disagreements might arise from problems in the measurement of damage width or fracture energy [144].

Experiments with various handsheets (i.e. paper hand-made in a test laboratory) demonstrate how such a damage width w_d depends on fibre properties such as the fibre length, strength, inter-fibre bonding and fibre segment activation. For example, when fibres were made shorter by cutting, w_d decreased with the mean fibre length (figure 31). One can also calculate (tediously) the fraction of broken fibres, which is of the order of 10%. Thus w_d results mostly from a complicated pull-out mechanism in paper, since fibres mostly do not break, and extends above l_f. This again demonstrates the presence of several lengthscales in paper mechanics, from the segment length to the fibre length, and then over to w_d. It also suffices to show the presence of strong 'self-averaging', since one can substitute all the possible measures of paper structure and disorder with one single quantity, w_d, which moreover is a simple function of l_f.

The fracture of paper also shows signs of the presence of various kinds of disorder. This has various origins. Even were the structure is completely homogeneous otherwise, there would be areal mass variations on the floc-scale. Neglecting that, the structure varies from the fibre-length scale downwards. This implies that in an idealized fibre, contained in a sheet, the stress-state varies locally as was pointed out already, so the likelihood of the fibre breaking at any point varies even if the strength is constant. Finally, the fibres have various levels of internal structure. For all these reasons plus history-effects such as different degrees of local drying and viscoelasticity, the strength of a fibre will be a random function.

For the sake of all these effects the fracture of paper presents all the variety that goes under the common name of statistical fracture mechanics. This includes the strength of samples, in the laboratory, and in the case of a normal user, as a quantity that has statistical variation.

The average resistance to fracture has various definitions such as maximum strain, maximum stress or fracture toughness. All these would be expected to reflect the statistical aspects of the processes that bring about the final failure of a piece of paper under external loading.

The statistics of strength in brittle materials are usually approached using either extreme order statistics or numerical simulations of models and related analytical models. It is not entirely clear whether paper can be considered 'quasi-brittle' or ductile in this sense: whether one should only find the most critical defect—however it may be defined. From the practical viewpoint, what matters most is the strength of a 'web' in situations such as paper-making and end-treatment and printing. Obviously, a sheet of copy paper does not need to be particularly strong under tension. However, one may of course argue that the strength statistics reveal something fundamental about the critical defects and the role of linear fracture mechanics.

Experimentally, the determination of the applicable statistical prescription is still rather unclear. In the case of brittle fracture key ideas relating to the possible probability distribution of sample strength derive from the size distribution(s) of flaws and the role of surface defects. The outcome should in the simplest possible cases be either the Gumbel (double-exponential, or Duxbury–Beale–Leath) or the celebrated Weibull distribution [149]. The available evidence has not been able to distinguish between these two candidates, so far [139, 150]. The situation is of course made less transparent by the fact that paper samples can have 'several defect populations', e.g. stemming from edge cracks and the bulk ones [151].

The question 'how does fracture in paper develops? can be addressed by two further statistical considerations: how does the damage accumulate, and what can one say about the geometry of cracks? Even on tearing a piece by hand one can witness these two phenomena: an audible sound is emitted due to crack advancement and the final crack path is not straight.

The decrease of the elastic modulus of a sample—or the increase of 'damage'—is often referred to in the fracture mechanics community as quasi-brittle behaviour. The tool for understanding this, for the physicist, is simple statistical mechanics models as fuse networks—electrical analogues of real fracture—and even more simplified 'fibre bundle models'. The essence of such thinking is the interplay of load sharing and stress enhancements versus shielding. If the fraction of still-load bearing elements is ρ, then the simplest expression for an increase in local stress is $\sigma = \sigma_0/(1-\rho)$. On a more elaborate level the next step is to postulate a crack size population $P(l)$, with all cracks of length l inducing a local stress enhancement (or some version thereof) $\sigma = f(\theta)1/\sqrt{r}$, where r is the distance to the crack tip. To balance this, the cracks also get shielded by the presence of others. These effects lead in practice to the well-known phenomenon of localization: even in the absence of plasticity the damage concentrates in a finite zone, in particular as measured in the direction in which the external stress is applied. In paper, such phenomenology is certainly observable. However, in contrast to some other materials such as concrete in which the elastic modulus can be observed to drop considerably prior to macroscopic failure, there is little proof for any finite drop in the sample elastic modulus from standard tensile tests.

A more sensitive technique to follow damage increase is AE (see figure 33). In paper as in other (brittle) media the released elastic energy is converted to sound waves and can be detected by piezoelectric transducers, among others. A part of it goes into heat and can be monitored via IR imaging as in others, e.g. glasses (see figure 32). The exciting questions here are what are the generic statistical features of the AE, and from a more practical viewpoint can these be related somehow to the fracture dynamics? It turns out that a tensile test yields results very similar to several other materials in the literature. In particular, the accumulated probability distribution of *acoustic event* energies follows a power-law form, $P_{\mathrm{AE}}(E) \sim E^{-\beta}$, with $\beta \sim 1.2 \pm 0.1$. This in turn tells us that the AE is not related to any particular 'microstructural scale of damage', such

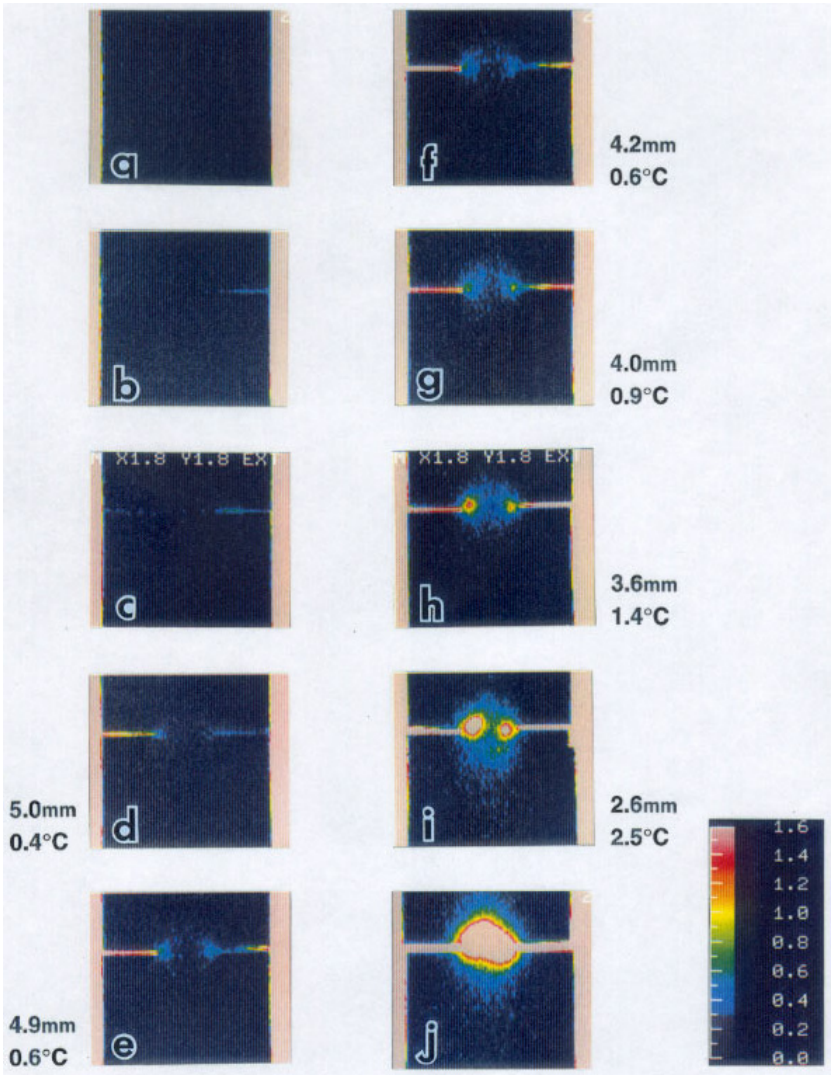

Figure 32. Infra-red images of temperature increases during crack propagation. A part of the released elastic energy or work done in failure goes into heating the material, which is manifested by the colour code used in the subfigures. Courtesy of A Tanaka (KCL).

as the failure of individual fibres or bonds, though contrasting claims do exist [152, 153]. The network relaxes in a coherent fashion, which means that any 'local element' fracture releases typically more elastic energy than expected (as can be also confirmed by simulations [154]). Unfortunately, there is little understanding of such exponents as β via simulations [50, 155, 156]. Typically, (brittle) fracture models would predict $\beta \sim 1.7$ or so, which is far off the measured one(s) [50, 156]. It is amusing to note that paper thus shows many of the features of earthquake statistics, such as Richter's law for energies and Omori's law for event intervals τ (figure 35).

The accumulation of AE energy in an experiment is related to the rather deep issue of the character of fracture from the statistical physics viewpoint. If $P(E)$ is power-law-like it is an attractive idea to relate this to a diverging scale, as the failure point is approached when strain or stress is increased (consider figure 34, which demonstrates how the AE energy can

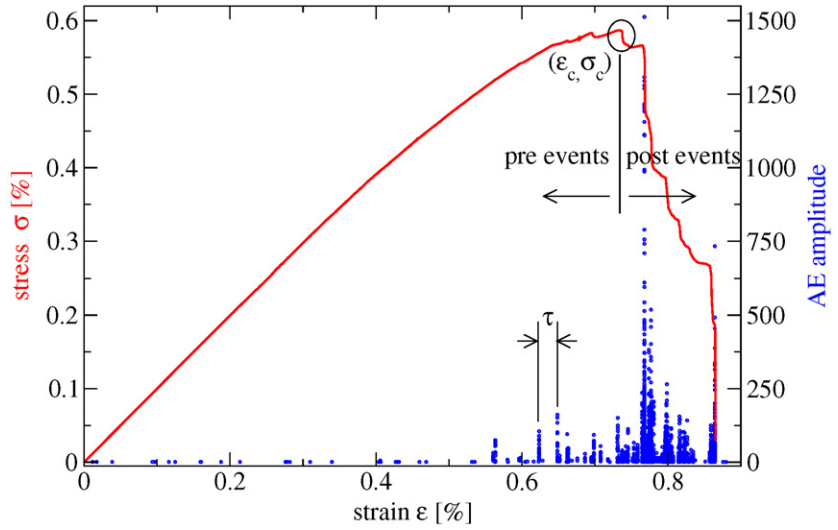

Figure 33. The stress–strain-curve and the AE are related in paper. At which part of the stress–strain-curve does the AE accumulation start? Courtesy of L Salminen, HUT.

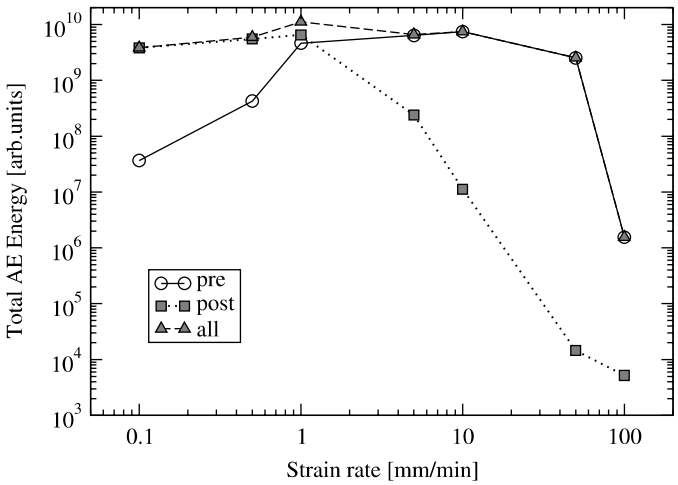

Figure 34. The fractions of AE energy, prior to and after the σ_c of the stress–strain curve, as a function of the strain rate in mode I experiments. As is clear, the behaviour of paper varies greatly, nevertheless the Gutenberg–Richter-like scaling of $P(E)$ is seen. Courtesy of L Salminen, HUT.

be distributed in paper fracture along the stress–strain curve). This scale would apply, e.g. to the volume from which individual AE events originate. This is in clear analogy to phase transitions in statistical mechanics, with a divergent correlation length. It is by no means clear in such a picture as to what would amount to an order parameter, in the sense of statistical mechanics. For example, the elastic modulus, in paper, definitely jumps to zero abruptly once the catastrophic crack growth takes place. There are some indications from other materials that the integrated AE energy might diverge close to the critical stress σ_c [48]. Likewise, Sornette and co-workers have tried to relate individual time-series of AE events to 'discrete scale-invariance', the birth and existence of a preferred scale in the fracture process [158]. Both

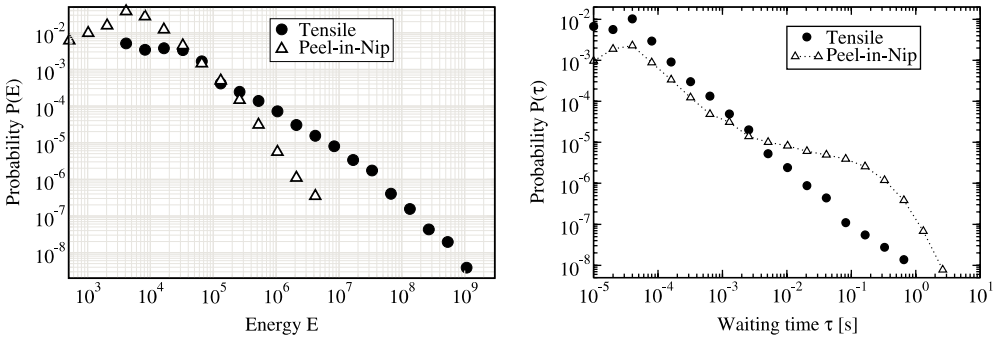

Figure 35. Left panel: the energy distribution $P(E)$ for two experimental set-ups. Both exhibit *power-law* statistics but with different exponents, and that of mode I has a much smaller exponent (close to 1.2). Right panel: the distribution of time intervals τ for mode I and in-plane experiments. Both obey an Omori's law-like scaling, and mode I one scales close to $P(\tau) \sim \tau^{-1}$. For the in-plane one there is a distinct time-scale related to the time it takes for the fracture line to cross an area related to the bond size [157].

these ideas do not fare well with the paper tensile AE data; in particular the accumulated AE energy is closest to an exponential function of the strain. The proper theoretical interpretation of such results is still missing [157].

A quantity that might be considered important in the context of crack energy consumption and is, moreover, very intriguing is the 'roughness' of cracks. For the last twenty years or so there has been some interest in the fractal or self-affine properties of fracture surfaces. Consider a crack path $h(x)$ and the associated scale-dependent mean-square fluctuation

$$w(l) = (\langle (h(x) - \bar{h}_l)^2 \rangle)^{1/2}, \tag{3}$$

where the local average height is to be computed inside each local window of length l. A signal of self-affine scaling is now the property that for the 'local width' one has

$$w(l) \sim l^{\chi}, \tag{4}$$

a power-law-like scaling relation, which also defines a roughness exponent χ. Other measures that would yield—for self-affine $h(x)$—such an exponent are the 'global width' or the limit $l \to L$ of $w(l)$, where L is the sample size, the scaling of power spectra of $h(x)$, two-point correlation functions of h and so forth. Perhaps the simplest possible such signal is given by the Brownian motion or a random walk, with $\chi = 1/2$ as indicated by the diffusion law $\langle (\Delta r)^2 \rangle = Dt$, where D is the diffusion constant.

Paper is rather unique as a material on which fractography experiments are done due to its two-dimensional nature as most of the literature on the self-affine roughness deals with three-dimensional samples [42, 160]. Various results on other materials [161] and paper [162–164] in the literature imply that the 2D crack geometry is 'superdiffusive', as the measured χ are in excess of the random walk value $1/2$. A part of the problem might be due to the fact that paper cracks are diffuse (figure 5). An example of a crack from a whole web from a paper machine is shown in figure 36. The resulting rougness can be seen in the corresponding figure 37.

These results are not understood as of now. The standard model of quasi-brittle fracture, the RFN, implies from the most recent simulations $\chi \sim 0.75$, in excess of most of the experiments. This model also implies *anomalous* scaling [155, 165] with which the various ways of computing the roughness exponent do not agree completely. Typically, the local and global measures differ, which implies the presence of (yet another) scale that changes with the measurement window size. For fuse networks the global exponent that can be found,

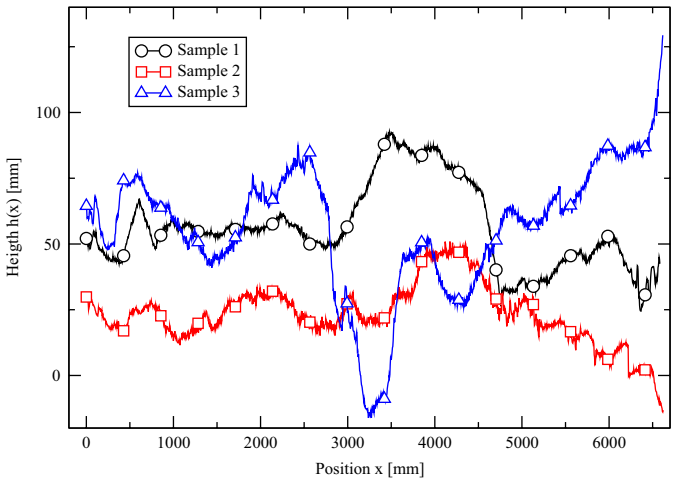

Figure 36. Fracturelines of a 6500 mm wide web break [159]. Three different cases are included.

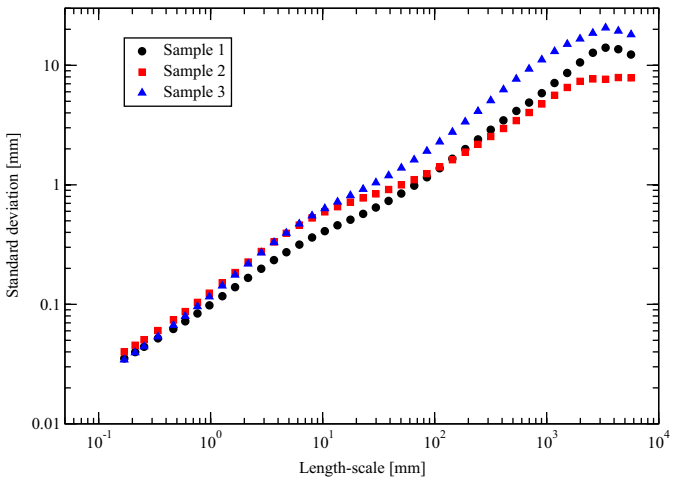

Figure 37. Roughening of the fractureline: the local fluctuations increase as a power-law of the measurement window size, which implies a self-affine profile with $\chi \sim 0.6$ [159]. Three different samples are depicted the same as in figure 36.

e.g. for fixed system sizes from the power spectrum or the structure factor is larger than 0.8. The question is, should this be true also for paper? In RFNs the fracture process is put on a discrete lattice, and the full elastic description is replaced by a scalar field. The main ingredient to match with paper is then the disorder, put in as locally varying failure thresholds for the couplings (fuses) between the lattice nodes. Perhaps technically closer to paper are the results of beam–network simulations of Skejtne *et al.* In these beams are substituted for fuses so more conventional elasticity is approached. The outcome is even less in-line with paper results, with χ seemingly depending on the particular disorder used and typically around 0.85 [166].

One possibility is that the ductility neglected in simulation models plays a crucial role. For scalar plasticity, the yield path (one-dimensional yield surface) has exactly a $\chi = 2/3$.

This result can be derived by noting first that the path minimizes its energy and then writing down the Hamiltonian

$$H_{\mathrm{MES}} = \int_0^L \gamma(\partial_x h(x))^2 + V(x, h(x))\,\mathrm{d}x, \tag{5}$$

where the first term is the (expanded) elastic energy, one with the elastic constant, γ, and the second, V, considers the frozen-in-place (from the viewpoint of a fracture test) variations in the yield energy. By standard techniques, $\chi = 1/z_{\mathrm{KPZ}} = 2/3$, where z is the dynamical exponent of the celebrated Kardar–Parisi–Zhang equation in non-equilibrium statistical mechanics [167]. An interpretation would be that $V(x, h)$ measures the local fracture toughness, and the fracture path manages to optimize the *integral* of the locally varying energy consumption that arises from V. Again, experiments produce various values of χ, often not equal to $2/3$.

Procaccia and co-workers have recently tried to combine an exact solution of rough single-crack elastic fields to void growth and resulting crack expansion, an idea that works precisely in 2D, two-dimensional stress-field and the role of damage [168]. Voids coalesce with the main crack, leading apparently to faster-than-diffusive deviatory behaviour, with a $\chi \sim 0.65$ or so. It is a good question whether the actual plasticity mechanisms (given the microstructure and so forth) are the same as in paper, and whether the diffuse crack surfaces would actually correspond to such a growth mechanism.

The connection with rough cracks and quantities of engineering interest can be made by considering the R-curve or the crack extension resistance. This means a generalized form of fracture toughness and in many fibre composites and paper forms an important part of the picture of material failure. The reason is often fibre pullout or *crack bridging* due to the presence of 'tough' fibres that hold the two crack faces together, though mesoscopically the crack tip has advanced beyond such local bridges (figure 5). One can now define a fractal picture of toughness, by considering the roughening in a coarse-grained sense. The idea is to compute more exactly δA, the increase in crack surface due to advancement. This starts in 2D (where $A \to l$) from the expanded version $l \sim \int 1 + \Delta^2 h(x)\,\mathrm{d}x$ and assuming h scales as in a self-affine fractal [169]. A more recent version by E Bouchaud and collaborators considers, again, anomalous scaling, due to the presence of an additional scale contributing to h. This increases as the crack propagates, and so the actual crack surface produced by the crack advancement is larger in the initial phases, with a concomitant increase in the energy consumption and thus an R-curve is born [170]. It is an open question if such ideas can be related to paper failure given its quasi-3D nature.

The statistical aspects of fracture can be also considered in the framework of creep or fatigue. Experiments on paper have not usually analysed generic 'non-paper' aspects of these issues. An exception is given by the work of Santucci *et al* where the 'jumps' of the crack tip in creep failure have been studied [171]. Qualitatively, the results show that the growth takes place via 'jumps' that grow with the length of the crack, which as such is not surprising since the process cannot be fully continous on a macroscopic scale. More interestingly the jump size distribution seems to obey a scaling form, whose explanation is an open issue. So also is the relation to the usual diffuse characteristics of fracture in paper, which makes an exact defect length establishment complicated (see figure 5). The 'stick–slip' motion of crack advancement in paper has been noted by many authors (e.g. see [172]) and is again, qualitatively, in analogy to the response of amorphous glasses to shear strains, related to the coarse-graining of elasticity mentioned earlier.

We finally mention one aspect where paper fracture mechanics has interesting twists: reinforcement. This term means as in composite science and technology the mixing of two 'ingredients', here pulps, to improve paper response such as stiffness or more usually fracture resistance. The usual scenario is such that cheap mechanical pulp is assisted with

more expensive chemical pulp, which in turn is more able to bond (due to fibre flexibility or conformability) and also more ductile (figure 21 shows an example of the strength versus volume fraction in a mixture).

As in composite mechanics, one may now ask the question how a single reinforcement fibre influences the stress-state of the network around it, and then move on to finite volume fractions. The expected outcome is in fibre networks complicated by the changing structure ('mixing two kinds of pasta'). It is interesting to note that in the case that the connectivity of the reinforcement fibres is important for fracture resistance, the problem is a percolation one in disguise. Fibres percolate in two dimensions (sheet plane) while undulating in the third one, so their flexibility is of importance (this changes the percolation limit from the 2D ideal case), and if a mixture of pulps/fibres is considered then the fibres may be 'shielded from contact' due to the other component [173].

4. Liquids in fibre networks

4.1. Mass flow

Imbibition and drainage are the two mirror images of dynamic phenomena that one uncovers if one considers the transport of fluids in porous media or multi-phase flows. They include as a 'special case' steady-state fluid flow. Paper provides an interesting example of a disordered pore network, in its bulk. One special case is liquid(s) on the surface which is discussed separately below.

In the low Reynolds number limit of Stokes' flow, the fundamental equation is the Darcy law. This reads

$$\langle \boldsymbol{q} \rangle = -\frac{\kappa}{\eta}(\boldsymbol{\nabla} P) \tag{6}$$

where $\langle \boldsymbol{q} \rangle$ is the average volume of fluid transported per unit time per unit cross-section, and κ and η are the *average* permeability and viscosity, respectively. The effective permeability is the only structural parameter used as an input.

The calculation of the permeability is a classical problem in transport theory, and is complicated here by the presence of the random structure. Geometrical considerations and effective medium theory allow approximating κ as a function of the porosity. For fibre networks with a random geometry, this is not so simple. There are estimates such as the Kozeny–Carman expression, which attempt to describe the coarse-grained behaviour with the aid of two parameters: the porosity and the internal pore surface area. This states that the permeability k is related to the porosity ϕ via

$$k = \phi^3/cS^2, \tag{7}$$

where S is the specific surface area of the porous medium. c is called the 'Kozeny constant' or 'Kozeny factor', which should be fitted separately for e.g. paper. This has been attempted approximately in various ways in the literature (see [174]). The expression also contains the rather free parameter S, which is difficult to estimate reliably for a material such as paper.

Equation (7) implies that the fluid flow decreases quickly with porosity, but the expression does not contain the *percolation* threshold of the pore structure. Thus for small enough porosities it has to be wrong. This exhibits the typical problem of effective-medium approaches for transport quantities as e.g. current, mechanical forces etc. The typical behaviour of $k(\theta)$ is depicted in figure 38. A corresponding example of a flow field from numerical simulations is provided in figure 39, such as was used to produce figure 38 as well.

Paper presents an interesting example of the connection of statistical geometry and transport theory. The question, in general is studied by looking at bounds for the quantity at

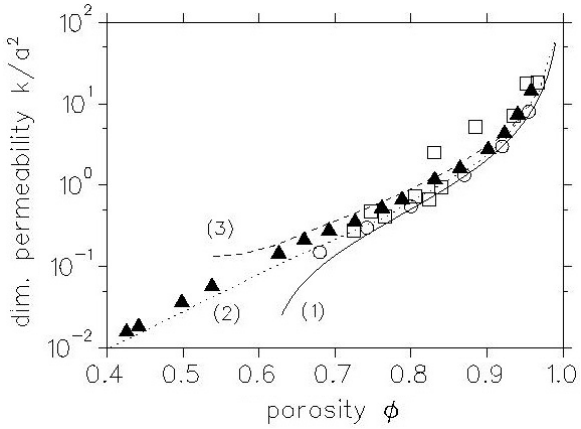

Figure 38. The simulated 'nondimensional permeabilities' k/a^2 as a function of porosity (black triangles). The boxes and circles are experimental results (see [174] for details, as well as for curves 1 and 2). Curve 3 is the Kozeny–Carman result (equation (7)), when S is computed from the structure simulations ([174]).

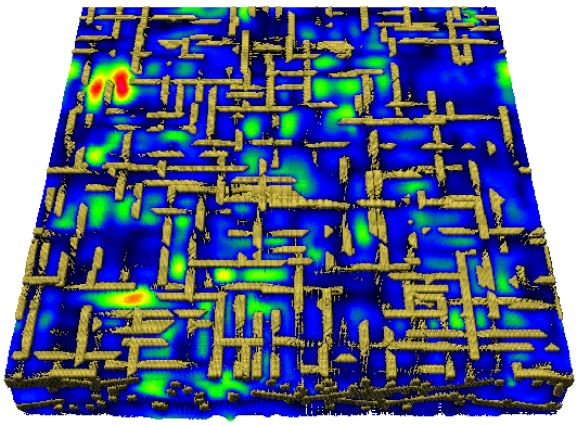

Figure 39. The out-of-plane velocity field of a simulated three-dimensional fibre network structure ([174]). Bright colours indicate high fluid velocities. How is the structure (including micron-scale effects as fibre surface roughness) reflected here and in real paper?

hand, obtained by using statistical measures (two-point correlations, three-point correlations, 'lacunarity' etc).

For the practically minded paper scientist the quest would then be for a minimal set of measurable parameters, such that the permeability could be estimated reliably and reasonably accurately. It would be important to understand what controls permeability; whether this is a result of the network structure only, or if fibre surface properties play a role.

The measurement of permeability in the case of paper is slightly tricky. The structure is compressible and thin. The development of the lattice-Boltzmann technique has made it possible to adapt microscopic boundary conditions that can follow—to some extent—the real ones. There are two basic approaches to this end. Either the discretized structure can be formed by simulations, as by the models discussed in section 2, or one can resort to tomographic 3D imaging, and export the data to a simulation model [175].

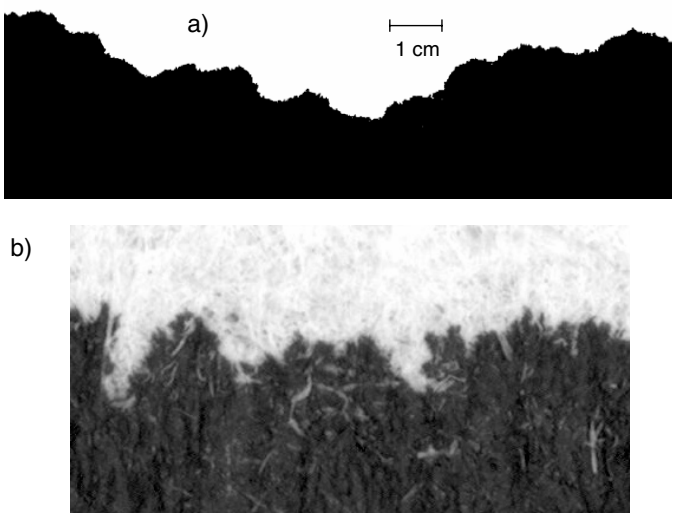

Figure 40. Front of black ink sucked into a paper towel. (*a*) digital photograph, ca 1200 pixels horizontal resolution, dark and light grey values were enhanced to black and white. (*b*) high resolution scan (1000 dots cm^{-1}) of a small part (ca 0.8 cm wide) in grey-scale. The structure of the medium, as the fibres on the paper top surface, and its effect on the fluid front becomes visible [12].

Detailed comparisons have been attempted in recent years. The most naive structure models give estimates of the 'out-of-plane' permeability that are far too high [174, 176, 177]. This is in spite of the fact that other porosity-related properties can be reproduced with some confidence. In other words, the 'tortuosity', the wiggling of the flow paths and patterns would be expected to reproduce reality. The most credible reason for the mismatch is the nano- and microscale roughness of the fibres. This modifies the no-slip boundary condition and forces much of the pore volume to assume the role of a stagnant zone, which does not contribute to fluid flows. It remains to be seen how quickly more elaborate imaging-based simulations can converge towards the experiments. Two issues that are interesting are whether the flow fields truly self-average (see figure 39 for a motivation) and the role of the swelling of the web structure.

4.2. Two-phase flows: imbibition

Imbibition and drainage are concerned with the removal of a liquid/gas by another one, and the essential difference is the viscosity ratio of these two liquids or a liquid and a gas. The typical physics is indicated by the Young–Dupré equation, applied to a drop of liquid on a solid surface. This reads as

$$\sigma_{s2} - \sigma_{s1} = \sigma \cos\theta, \tag{8}$$

where σ_{s1} and σ_{s2} are the surface tensions of the solid with fluids 1 and 2, respectively. The contact angle θ determines whether liquid 1 is wetting ($\theta < \pi/2$) or non-wetting ($\theta > \pi/2$). The former case is met in imbibition. This is what we, in the following, mostly concentrate on. It is the most studied phenomenon in the paper context. An example of ink penetration into paper is shown in figure 40.

Drainage is, in the statistical physics literature, often most discussed in terms of two concepts: viscous fingering and invasion percolation. These combine two ideas. The 'front'

is inherently unstable, and will undergo a fingering instability. However, this is modified by the presence of the pore structure. The fact that in a disordered porous medium the less viscous fluid appears to penetrate without any effective surface tension (as such instabilities take place) implies that what matters is the statistics of porosity: a breakthrough of the invading fluid occurs utilizing the fraction of the pores that is connected and accessible.

In paper-related practical applications things may be complicated by the presence of inks and other more complicated liquids (that contain surfactants, in general). Also, as in many other contexts the value of θ may have a *dynamical* origin, related e.g. to whether the three-phase boundary is advancing or receding [180, 181]. The liquid that penetrates can be non-Newtonian, when, essentially, the consequences are not understood [182, 183]. For instance ink, of all the liquids met in the context of paper, provides an example [184]. It is easy to envision complications that arise due to the specific geometry of fibre networks. These are discussed below. In paper, one also meets interesting changes to usual behaviour, caused by the time-dependent interaction between the invading phase and the fibre network. Or, the 'treatment' of paper may lead to a build-up of sedimented material that is carried with the liquid, thus again changing the pore structure [185, 186].

Due to the anisotropic nature of paper the penetration of liquids in to an empty pore space can be considered essentially in two cases: out-of-plane and along the sheet plane. The former involves very small quantities of liquid and can directly be seen to depend much on the surface roughness and the details of the pore network. Meanwhile, it also has to do with classical droplet spreading issues. The question of droplets on permeable, rough surfaces is a tough nut to crack [187].

In imbibition, there are two basic setups: driven (external pressure) versus spontaneous. The latter is known as the Washburn–Lucas–Rideal law, $h \sim At^{1/2}$ for the length of a capillary tube invaded—a classical result for the timescales [188]. The same result, the square-root law, often holds in a coarse-grained sense. When this is true, the question arises whether the prefactor A (and the initial deviations from the law) can be explained, and when it is not true, what microscopic reason could there be for the failure of the Washburn law [12].

In paper, the scaling properties of wetting liquid intake are bewildering. Due to the scales involved, penetration perpendicular to the sheet is difficult to observe compared with the in-plane one. See figure 41 for a schematic drawing of the various in-plane complications. Observations of the timescales involved imply that spontaneous imbibition in this case can obey various scalings. That is, $h \sim t^{\alpha}$ with $\alpha = 0, \ldots, 1$. Notice that in-plane 'driven imbibition' is fundamentally hard to set up. The underlying reasons are similar to e.g. imbibition in the context of oil recovery: one should be able to establish an external pressure difference which is large compared with the capillary pressures involved.

The square-root law implies that local piston-like pore-scale penetration can be upscaled. This can fail when the dynamics is governed by precursor layers. These wet in advance the pore surfaces, and should this take place at a rate faster than expected it is clear that the intake can actually follow $\alpha > 1/2$. The snap-off of pores (which get filled by expanding films on the pore walls) follows a non-linear diffusion equation on the microscopic level. Further, the usual assumption is that the effective dynamical contact angle is a constant. If it depends on time, it is clear that the process can change its rate rather arbitrarily. In sized papers this would be a real possibility, while in hydrophobic/philic papers the contact angle would be a constant. There are many different scales involved. These start from 0.1–1 mm (largest pores) and extend down to fibre wall micropores and the lumen. The complicated geometry of pores may give rise to rate-defining processes, as menisci get pinned at discontinuities [189, 190], and lead to the question what is the right 'pore size', or the right capillary diameter [191].

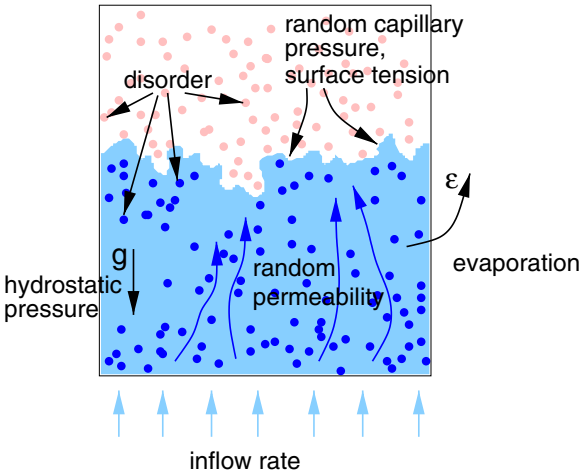

Figure 41. Schematic representation of elementary processes involved in quasi-two-dimensional imbibition. Courtesy of Martin Rost, University of Bonn.

There are two other ways of looking at the penetration of liquids relevant to paper, both involving more elaborate physics. The classical transport-in-porous-media approach is to consider the saturation profiles [192–196]. Such data indicates that the fluid enters the fibre network so that there is a 'front' behind which the remaining air is reduced slowly. This is true in many other porous media problems where the so-called Richard's equation is often used: it involves a complicated saturation-dependent diffusivity for the saturation (fraction of fluid-occupied pore space). These ideas are made much more elaborate by the the presence of two effects: water intake by the fibre walls and swelling. The former acts as a sink of liquid (and is of profound importance in paper-making during drying). The latter makes the structure of the network time-dependent in a non-trivial manner [197–199]. This is illustrated in figures 42 and 43 which deal with 'fibre plugs', i.e. not directly paper but with larger volumes to overcome measurement limitations with NMR [178].

A fundamental physics question that such approaches neglect is: 'what is the thermodynamic driving force?'. Recall that in the coarse-grained Washburn-law one has a capillary pressure as well. Where and how is this to be computed, if a medium has locally varying saturation, or in other words, where are the pores where the movement of meniscus creates the main mass flow? A rather usual implicit assumption is that this question is answered by distinct fronts which also correspond to the intutitive picture (figure 40). Experiments have shown [179] that both the optically determined front and the mass-intake can follow Washburn-laws, with different prefactors (figure 44).

Such fronts $h(x)$ also *roughen*, in the same manner as cracks in paper. The process here is such that three crucial ingredients can be listed: (i) the slowing-down of the interface (front) and its dynamics due to the Washburnian behaviour (though as a complication the front average position often varies from the square-root dependence on time). Then, (ii) there is intrinsic disorder, the intriguing pattern formation (figure 40) would not take place here without it. And, (iii) from the theoretical viewpoint it is interesting that the fluid conservation will saturate the roughening at a related scale. This is a consequence of the fact that the front curvature will at some point stop developing thanks to the conservation of liquid, so that a scale $\xi_\times \sim h^{1/2}$ develops in, for instance, spontaneous imbibition, regardless of any other detailed considerations. This can be argued for by elaborate phase-field models [12, 200], by

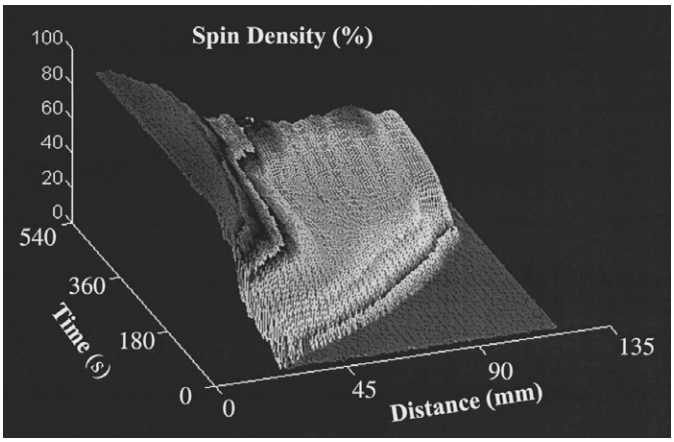

Figure 42. Saturation profiles of the liquid in a fibre assembly (plug) [178], as a function of time and distance from the liquid reservoir. Note that the change in saturation from dry to fully saturated is gradual.

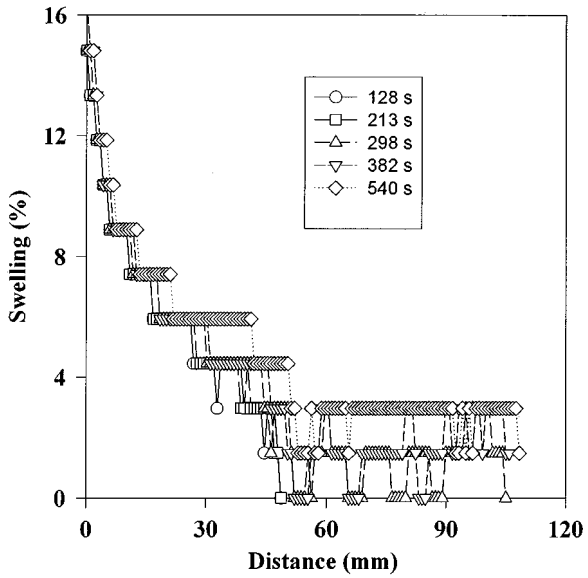

Figure 43. The swelling of fibres, as a function of time and distance, in a 'plug' (see [178]). A concomitant change in local permeability, and thus local fluid flow, is expected.

simple considerations [201], and finally it has been confirmed by experiment [202]. Currently there are many results related to front 'kinetic' roughening in paper, but little quantitative understanding in terms of exponents such as the χ met earlier ([203–208], see also [12] for a review). Such 'theory' may be of practical interest in e.g. printing, since the liquid penetration will be uneven [209].

Another imbibition-like problem is that of a liquid drop on the surface. What happens? The basic physics is two-fold: penetration into and spreading on the surface. The so-called Tanner's law is what would describe the latter on an ideal surface. Now, for real surfaces the contact line between the drop and the dry surface gets pinned locally due to surface roughness

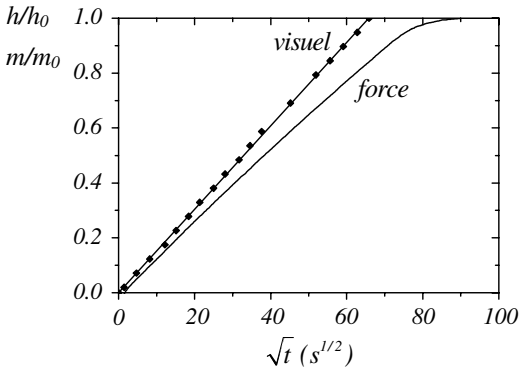

Figure 44. The front and the mass (of the silicone fluid) in a paper sample versus time (Washburn-scaling, $\sim t^{1/2}$), according to [179]. The implication is that the saturation is incomplete behind the front.

(pits, undulations etc). The surface variation means that the effective contact angle is not a constant. This physics is not well understood even in more controlled contexts. 'Naked eye' experiments confirm the presence of more complicated effects: there are thin films forming precursors. One can again imagine still more complicated scenarios for droplet spreading such as involving the use of shear-thinning liquids. Recently, the imbibition of a droplet on a deforming substrate has drawn interest [210]. The paper-related application is the dual problem of penetration into the bulk, and spreading on a surface complicated by deformations and possibly viscous dissipation [211–215]. This is not very well understood either, but is directly related to the question of the sharpness of print: how a single printed character (say) shapes up on the paper surface from the printing process. In engineering language this goes by the name of 'print mottle'.

5. Final remarks

We hope to have demonstrated that the physics of paper is interesting and versatile. Paper is a readily available but still very complicated material which provides a testing ground for the theories of disordered materials. A good understanding of paper properties serves the purpose of enhancing the usability of paper products. Based on renewable wood raw material, paper and board give sustainable solutions to information transfer and packaging. Research on the physics of paper allows the papermakers to use wood raw material more efficiently, develop leaner sheet structures and improve the performance of paper products.

The efforts of understanding the physical properties of paper have led us to understand how to treat the disordered fibre network structure where every fibre is different. Papermakers today can manufacture papers with very different network structures and physical properties. In spite of the large variability, we can still explain many of the properties of paper with simple average or 'mean-field' models. Just consider the optical or mechanical properties. In optics, the average microscopic free surface area governs the macroscopic light scattering coefficient (figure 3) even though one might expect that the multiple scattering and transmission events would be sensitive to structural correlations in the thickness direction of the sheet. Likewise, the tensile strength of paper seems to be insensitive to the in-plane disorder of the sheet and of the statistics of the fracture process, such as the self-affine character and the roughness exponent of the fracture line ([160]). Clearly, we do not understand why the averaging works as well as it does.

The transport properties of paper and its dynamic interaction with water is the most important largely unexplored area of paper physics. The macroscopic (into fibre network) and microscopic (into fibre wall) penetration mechanisms, the concurrent dimensional changes, and the interaction of water molecules with the polymeric and crystalline structures of fibre wall material are all topics of high interest. Another area largely overlooked is the clustering and deposition processes that give rise to the geometric organization of filler, fine particles, colloidal polymers and the fibres themselves during the hydrodynamic sheet formation process.

The third 'unexplored territory' which we would like to point out is the mechanical defibration process. In order to be able to make paper out of wood, the fibres in wood must be separated and beaten to increase their conformability. The process of mechanical defibration depends on the rheology of the fibrous structure of wood. As this is a major consumer of energy, it would be important to understand what happens in the mechanical defibration process. The challenges lie with the disorder of wood material which ranges from the microscopic structure of individual fibres (just as in paper) to the organization and variability of the fibres over macroscopic distances in wood.

The quest to develop better paper products is highly relevant in the modern world. For example, better wood-fibre based packaging materials will give food better protection. This contributes to the fight against hunger in the world. The biosynthesis of wood fibres uses carbon dioxide from air. When using paper materials, one fights the global climate change.

Acknowledgments

MJA would like to thank the Academy of Finland, including its Center of Excellence-program, and TEKES (The National Technology Agency of Finland) for financial support. A number of students, colleagues and partners in research (E Hellén, V Räisänen, L Salminen, E Seppälä, J Rosti, M Dubé, M Rost, J Lohi) are thanked for collaborations and discussions concerning the physics of paper. KJN is deeply grateful to the many individuals in the Finnish forest cluster and TEKES whose support has made possible the research of paper physics in Finland and to numerous students and colleagues for the fruitful collaborations. In addition to the co-author, D Gunderson, H Kettunen, J Ketoja, M Leskelä and R Wathén have played a major role.

References

[1] Niskanen K J (ed) 1998 *Paper Physics* (Helsinki: Fapet)
[2] Hollmark H, Andersson H and Perkins R W 1978 *J. Tappi* **61** 69
[3] Page D H and Schulgasser K 1989 Evidence for a laminate model for paper *Mechanics of Cellulosic and Polymeric Materials* ed R W Perkins AMD-vol 99
Page D H and Schulgasser K 1989 Evidence for a laminate model for paper *Mechanics of Cellulosic and Polymeric Materials* ed R W Perkins MD-vol 13
[4] Head D A, Levine A J and MacKintosh F C 2003 *Phys. Rev. Lett.* **91** 108102
[5] Wilhelm J and Frey E 2003 *Phys. Rev. Lett.* **91** 108103
[6] Jacobs D and Thorpe M F 1995 *Phys. Rev. Lett.* **75** 4051
Moukarzel C and Duxbury P M 1995 *Phys. Rev. Lett.* **75** 4055
Moukarzel C, Duxbury P M and Leath P L 1997 *Phys. Rev. Lett.* **78** 1480
[7] Alava M, Duxbury P, Moukarzel C and Rieger H 2001 *Phase Transitions and Critical Phenomena* vol 18 ed C Domb and J L Lebowitz (San Diego: Academic)
[8] Myllys M, Maunuksela J, Alava M, Ala-Nissila T, Merikoski J and Timonen J 2001 *Phys. Rev.* E **64** 036101
[9] Maunuksela J, Myllys M, Kähkönen O-P, Timonen J, Provatas N, Alava M J and Ala-Nissila T 1997 *Phys. Rev. Lett.* **79** 1515
[10] Krug J 1997 *Adv. Phys.* **46** 139
[11] Meakin P 1998 *Fractals, Scaling and Growth Far from Equilibrium* (Cambridge: Cambridge University Press)
[12] Alava M, Dubé M and Rost M 2004 *Adv. Phys.* **53** 83

[13] Corte H 1982 *Handbook of Paper Science* vol 2 ed H F Rance (Amsterdam: Elsevier) chapter 9
[14] Hellén E, Ketoja J, Niskanen K and Alava M 2002 *J. Pulp Pap. Sci.* **28** 55
[15] Bandyopadhyay A, Ramarao B V and Ramaswamy S 2002 *Colloids Surf.* A **206** 455
[16] Niskanen K J (ed) 1998 *Paper Physics* (Helsinki: Fapet) chapter 9
[17] For generic overviews of testing physical properties of paper, see 2001 *Handbook of Physical Testing of Paper* vol 1 and 2, ed J Borch and M B Lyne (New York: Dekker)
[18] Murphy E J 1960 *J. Phys. Chem. Solids* **16** 115
[19] Williams M 1993 The physics and technology of xerographic processes (Malabar, FL: Krieger Publishing Company)
[20] Sundholm J (ed) 1999 *Mechanical Pulping* (Helsinki: Fapet)
[21] Deng M and Dodson C T J 1994 *Paper—An Engineered Stochastic Structure* (Atlanta, USA: TAPPI Press)
[22] Vidal D, Zou X J and Uesaka T 2003 *Tappi* **2:3** 3
Vidal D, Zou X J and Uesaka T 2003 *Tappi* **2:4** 16
[23] See e.g. Andrade J S Jr, Herrmann H J, Andrade R F S and da Silva L R 2005 *Phys. Rev. Lett.* **94** 018702
[24] Edwards S F and Grinev D V 1998 *Phys. Rev.* E **58** 4758
[25] Carlsson J, Hellentin P, Malmqvist L, Persson A, Persson W and Wahlström C G 1995 *Appl. Opt.* **34** 1528
[26] Niskanen K J (ed) 1998 *Paper Physics* (Helsinki: Fapet) chapter 4
[27] Granberg H, Rundlof M and Mattsson L 2003 *J. Pulp Pap. Sci.* **29** 247
[28] Green K, Lamberg L and Lumme K 2000 *Appl. Opt.* **39** 4669
[29] Alince B, Porubska J and Van De Ven T G M 2002 *J. Pulp Pap. Sci.* **28** 315
[30] Fellers C, Andersson H and Hollmark H 1986 The definition and measurement of thickness and density *Paper—Structure and Properties* ed J A Bristow and P Kolseth (New York: Marcel Dekker) pp 151–68
[31] Norman B 1989 Overview of the physics of forming *Fundamentals of Papermaking* vol 3 ed C F Baker and V W Punton (London: Mechanical Engineering Publications) pp 73–149
[32] Snoeijer J H, van Hecke M, Somfai E and van Saarloos W 2004 *Phys. Rev.* E **70** 011301
[33] Blair D L and Kudrolli A *Preprint* cond-mat/0412678
[34] Houle P A and Sethna J P 1996 *Phys. Rev.* E **54** 278
[35] Mark R E and Gillis P P 1983 Mechanical properties of fibers *Handbook of Physical and Mechanical Testing of Paper and Paperboard* vol 1 ed R E Mark (New York: Dekker) pp 409–96
[36] Campbell W B 1959 *Tappi* **42** 999
[37] Page D H, Tydeman P A and Hunt M 1962 A study of fibre-to-fibre bonding by direct observation *The Formation and Structure of Paper* vol 1 ed F Bolam (London: BPBMA) pp 171–94
Nanko H, Ohsawa J and Okagawa A 1989 *J. Pulp Pap. Sci.* **15** J17
[38] Davison R W 1972 *Tappi* **55** 567
[39] Luner P, Kärnä A E U and Donofrio C P 1961 *Tappi* **44** 409
[40] Niskanen K J 1993 Strength and fracture of paper *Tenth Fundamental Research Symp. (Oxford, UK, September)* pp 641–725
[41] See e.g. chapters by Hansen A, Duxbury P and de Arcangelis L 1990 *Statistical Models for the Fracture of Disordered Media* ed H J Herrmann and S Roux (Amsterdam: North-Holland)
[42] Bouchaud E 1997 *J. Phys. Cond. Mat.* **9** 4319
[43] Fineberg J and Marder M 1998 *Phys. Rep.* **313** 1
[44] Kettunen H and Niskanen K 2000 *J. Pulp Pap. Sci.* **26** 35
[45] Sethna J P, Dahmen K A and Myers C R 2001 *Nature* **410** 242
[46] Lockner D A, Byerlee D, Kuksenko V, Ponomarev A and Sidorin A 1991 *Nature* **350** 39
[47] Petri A, Paparo G, Vespignani A, Alippi A and Costantini M 1994 *Phys. Rev. Lett.* **73** 3423
[48] Guarino A, Garcimartin A and Ciliberto S 1998 *Eur. Phys. J.* B **6** 13
Garcimartin A, Guarino A, Bellon L and Ciliberto S 1997 *Phys. Rev. Lett.* **79** 3202
[49] Krysac L C and Maynard J D 1998 *Phys. Rev. Lett.* **81** 4428
[50] Salminen L I, Tolvanen A and Alava M J 2002 *Phys. Rev. Lett.* **89** 185503
[51] Prahl J M 1968 Thermodynamics of paper fiber and water mixtures *PhD thesis* Harvard University Cambridge, MA
[52] Chatterjee S G, Ramarao B V and Tien C J 1997 *J. Pulp Pap. Sci.* **23** J366
[53] Dionne I, Werbowyj R S and Gray D G 1991 *J. Pulp Pap. Sci.* **17** J123
[54] Scallan A M 1974 *Wood Sci.* **6** 266
[55] Gallay W 1973 *Tappi* **56** 54
[56] Barkas W W 1951 *The Swelling of Wood under Stress. A Discussion of its Hygroscopic, Elastic and Plastic Properties* (London: H. M. Stationery Office)
[57] Uesaka T and Qi D 1994 *J. Pulp Pap. Sci.* **20** J175

[58] Uesaka T 1994 *J. Mater. Sci.* **29** 2373
[59] Brecht W 1962 Effect of structure on major aspects of paper behaviour with fluids *The Formation and Structure of Paper* ed F Bolam (London: BPBMA) pp 427–60
[60] Niskanen K J, Kuskowski S J and Bronkhorst C A 1997 *Nordic Pulp Pap. Res. J.* **12** 103
[61] Niskanen K J and Alava M J 1994 *Phys. Rev. Lett.* **73** 3475
[62] Kallmes O J and Corte H 1960 *Tappi* **43** 737
Kallmes O J and Corte H 1961 *Tappi* **44** 448
[63] Pike G E and Seager C H 1974 *Phys. Rev.* B **10** 1421
[64] Stauffer D and Aharony A 1994 *Introduction to Percolation Theory* (London: Taylor and Francis)
[65] Provatas N, Haataja M, Seppälä E, Majaniemi S, Åström J, Alava M and Ala-Nissilä T 1997 *J. Stat. Phys.* **87** 325
[66] Kerekes R and Schell C J 1992 *J. Pulp Pap. Sci.* **18** J32
[67] Kiviranta A and Dodson C T J 1995 *J. Pulp Pap. Sci.* **21** J397
[68] Schmid C F and Klingenberg D J 2000 *Phys. Rev. Lett.* **84** 1515
[69] Switzer L H, Klingenberg D J and Scott C T 2004 *Nordic J. Pulp Pap. Sci.* **19** 434
[70] Sampson W W, McAlpin J, Kropholler H W and Dodson C T J 1995 *J. Pulp Pap. Sci.* **21** J422
[71] Aidun C 1998 *Tappi* **81:5** 124
[72] Haglund L, Norman B and Wahren D 1974 *Svensk Papperstid* **77** 362
[73] Provatas N, Alava M J and Ala-Nissilä T 1996 *Phys. Rev.* E **54** R36
[74] Provatas N, Haataja M, Asikainen J, Majaniemi S, Alava M and Ala-Nissila T 2000 *Colloids Surf.* A **165** 209
[75] Kellomäki M and Jetsu P 2002 Measurement of floc size and sharpness using second-order statistics of grammage map *Progress in Paper Physics Seminar (Syracuse, NY)* pp 149–55
[76] Kellomäki M and Jetsu P Graininess of formation 2003 *Int. Paper Physics Conf. (Victoria BC Canada)* PAPTAC 2003 pp 193–9
[77] Niskanen K J 1989 Distribution of fibre orientations in paper *Fundamentals of Papermaking* vol 1 ed C F Baker and V W Punton (London: Mechanical Engineering Publication Ltd) pp 275–308
[78] Mecke K R, Arns C H and Knackstedt M A 2004 *Colloids Surf.* A **241** 351
Arns C H, Knackstedt M A, Pinczewski W V and Mecke K R 2001 *Phys. Rev.* E **63** 031112
[79] Hellén E K O, Alava M J and Niskanen K J 1997 *J. Appl. Phys.* **81** 6425
[80] Niskanen K and Rajatora H 2002 *J. Pulp Pap. Sci.* **28** 228
[81] Torquato S 2001 *Random Heterogeneous Materials* (Berlin: Springer)
[82] Vinnurva J, Alava M J, Ala-Nissilä T and Krug J 1998 *Phys. Rev.* E **58** 1125
[83] Schimschack M and Krug J 1995 *Phys. Rev.* B **52** 8550
[84] Lobosco V and Kaul V 2001 *Nordic Pulp Pap. Res. J.* **16** 313
[85] Kataja M, Hiltunen K and Timonen J 1992 *J. Phys. D: Appl. Phys.* **25** 1053
[86] Of course, the problem is highly non-trivial See, e.g. Le Corre S, Caillerie D, Orgeas L and Favier D 2004 *J. Mech. Phys. Solids* **52** 395
[87] Liu C-h, Nagel S R, Schecter D A, Coppersmith S N, Majumdar S, Narayan O and Witten T A 1996 *Science* **269** 513
[88] Sirviö J, Nurminen I and Niskanen K 2003 A method for assessing the consolidating effect of fines on the structure of paper *Int. Paper Physics Conf. (PAPTAC 2003) (Victoria BC Canada, 7–11 September 2003)* pp 187–92
[89] Bristow J A 1986 The paper surface in relation to the network *Paper—Structure and Properties* ed J A Bristow and P Kolseth (New York: Dekker) pp 169–82
[90] Retulainen E, Moss P and Nieminen K 1993 Effect of fines on the properties of fibre networks *Products of Papermaking* vol 2 ed C F Baker (Leatherhead: Pira International) pp 727–70
[91] Steffner O, Nylund T and Rigdahl M 1998 *Nordic Pulp Pap. Res. J.* **13** 68
[92] He J, Batchelor W J and Johnston R E 2004 *Appita* **57** 292
[93] Corte H 1982 The porosity of paper *Handbook of Paper Science* vol 2 ed H F Rance (Amsterdam: Elsevier) chapter 6
[94] Hyväluoma J, Raiskinmäki P, Jäsberg A, Koponen A, Kataja M and Timonen J 2004 *Future Gen. Comput. Syst.* **20** 1003
[95] Samuelsen E J, Gregersen O W, Houen P J, Helle T, Raven C and Snigirev A 2001 *J. Pulp Pap. Sci.* **27** 50
[96] Huang S, Goel A, Ramaswamy S, Ramarao B V and Choi D 2002 *Appita* **55** 230
[97] Holmstad R, Antonie C, Nygård P and Helle T 2003 *Pulp Pap. Canada* **104** 47
[98] Holmstad R, Ramaswamy S, Goel A, Gregersen O W and Ramarao B V 2003 Comparison of 3D structural characteristics of high and low resolution x-ray microtomographic images of paper and board 2003 *Int. Paper Physics Conf. (PAPTAC 2003) Victoria, Canada* p 65

[99] Seppälä E, Alava M and Niskanen K 1996 *Paperi ja Puu* **78** 446
[100] Provatas N and Uesaka T 2003 *J. Pulp Pap. Sci.* **29** 332
[101] Kortschot M T 1997 The role of the fibre in the structural hierarchy of paper *The Fundamentals of Papermaking Materials, The Eleventh Fundamental Research Symp. (21–26 September 1997)* (Cambridge: Pira International) pp 351–94
[102] Page D H, Tydeman P A and Hunt M 1962 A study of fibre-to-fibre bonding by direct observation *The Formation and Structure of Paper* vol 1 ed F Bolam (London: BPBMA) pp 171–94
Page D H, Tydeman P A and Hunt M 1962 Behaviour of fibre-to-fibre bonds in sheets under dynamic conditions *The Formation and Structure of Paper* vol 1 ed F Bolam (London: BPBMA) pp 249–64
[103] Nanko H and Ohsawa O 1989 Mechanisms of fibre bond formation *Fundamentals of Papermaking* ed Baker C F and Punton V W (London: Mechanical Engineering Publication Ltd) pp 783–822
[104] Niskanen K 2000 Kraft fibers in paper—Effect of beating *10th Int. Conf. CELLUCON 98* (Cambridge, UK: Woodhead Publication) pp 249–60
[105] Seth R S and Page D H 1983 The stress-strain curve of paper *The Role of Fundamental Research in Paper Making* vol 1 ed J Brander (London: Mechanical Engineering Publication) pp 421–54
[106] Götẗsching L and Baumgarten H L 1976 Tri-axial deformation of paper under tensile load *The Fundamental Properties of Paper Related to its Uses* vol 1 ed F Bolam (London: BPBIF) pp 227–49
[107] Haslach H W 2000 *Mech. Time depend. Mater.* **4** 169
[108] Niskanen K J (ed) 1998 *Paper Physics* (Helsinki: Fapet) chapter 7
[109] Courtesy of Aalto M ref. [1], Ch. 5
[110] Cox H L, Br. 1952 *J. Appl. Phys.* **3** 72
[111] For shear-lag models for discontinuous fiber composites, see Robinson I M and Robinson J M 1994 *J. Mater. Sci.* **29** 4663
[112] Räisänen V I, Alava M J, Niskanen K J and Nieminen R M 1997 *J. Mater. Res.* **12** 2725
[113] Åström J, Saarinen S, Niskanen K and Kurkijärvi J 1994 *J. Appl. Phys.* **75** 2383
[114] Åström J A, Mäkinen J-P, Alava M J and Timonen J 2000 *Phys. Rev.* E **61** 5550
[115] Wang C W and Sastry A M 2000 *Trans. ASME* **122** 460
[116] Milton G W 2001 *The Theory of Composites* (Cambridge: Cambridge University Press)
[117] DiDonna B A and Lubensky T C *Preprint* cond-mat/0506456
[118] Hristopulos D T and Uesaka T 2004 *Phys. Rev.* B **70** 064108
[119] Van Den Akker J A 1962 Some theoretical considerations on the mechanical properties of fibrous structures *The Formation and Structure of Paper* vol 1 ed F Bolam (London: BPBMA) pp 205–45
[120] Salminen L I, Alava M J, Heyden S, Gustafsson P-J and Niskanen K J 2002 *Nordic Pulp Pap. Res. J.* **17** 105
[121] Jentzen C A 1964 *Tappi* **47** 412
Dumbleton D F 1972 *Tappi* **55** 127
Giertz H W and Roedland H 1979 Elongation of segments—bonds in the secondary regime of the load/elongation curve *Int. Paper Physics Conf. CPPA* (Montreal) p 129
[122] I'Anson S 1997 *Paper Technol.* **38** 43
[123] Nissan A H and Batten G L *Tappi* **70** 119
Nissan A H and Batten G L *Tappi* **70** 128
Nissan A H and Batten G L 1987 *Tappi* **70** 137
[124] Lehti S T, Ketoja J A and Niskanen K J 2003 Measurement of paper rheology at varied moisture contents *Int. Paper Physics Conf. (PAPTAC 2003) (Victoria BC Canada 7–11 September 2003)* pp 57–60
[125] Jantunen J 1985 Visco-elastic properties of wet webs under dynamic conditions *Papermaking Raw Materials* vol 1 ed V Punton (London: Mechanical Engineering Publication) pp 133–64
[126] Skowronski J and Robertson A A 1986 *J. Pulp Pap. Sci.* **12** J20
[127] Andersson O and Sjöberg L 1953 *Svensk Papperstid.* **56** 615
[128] Gates E R and Kenworthy I C 1963 *Paper Technol.* **4** 485
[129] Padanyi Z V 1993 Physical aging and glass transition: effects on the mechanical properties of paper and board *Products of Papermaking* vol 1 ed C F Baker (Leatherhead: Pira International) pp 521–45
[130] Kolseth P and de Ruvo A 1983 The measurement of visco-elastic behavior for the characterization of time-, temperature- and humidity dependent properties *Handbook of Physical and Mechanical Testing of Paper and Paperboard* vol 1 ed R E Mark (New York: Dekker) pp 255–322
[131] Some papers on this approach are Falk M L and Langer J S 1998 *Phys. Rev.* E **57** 7192
Langer J S 2001 *Phys. Rev.* E **64** 011504
[132] Baret J C, Vandembroucq D and Roux S 2002 *Phys. Rev. Lett.* **89** 195506
[133] Korteoja M J, Lukkarinen A, Kaski K, Gunderson D E, Dahlke J L and Niskanen K J 1996 *Tappi* **79** 211
[134] Miguel M C, Vespignani A, Zaiser M and Zapperi S 2002 *Phys. Rev. Lett.* **89** 165501

[135] Nechad H, Helmstetter A, El Guerouma R and Sornette D 2005 *Phys. Rev. Lett.* **94** 045501
[136] Considine J M, Gunderson D E, Thelin P and Fellers C 1989 *Tappi* **82** 131
[137] Brezinski J P 1956 *Tappi* **39** 116
[138] Lavrykov S A, Ramarao B V and Lyne O L 2004 *Nordic Pulp Pap. Res. J.* **19** 183
[139] Korteoja M, Salminen L I, Niskanen K J and Alava M J 1998 *Mater. Sci. Eng.* A **248** 173
[140] Niskanen K, Mäkinen J, Ketoja J, Kananen J and Wathén R 2003 *Paperi ja Puu* **85** 274
[141] Korteoja M J, Niskanen K J, Kortschot M T and Kaski K K 1998 *Paperi ja Puu* **80** 364
[142] Niskanen K J, Kärenlampi P and Alava M J 1996 *J. Pulp Pap. Sci.* **22** J392
[143] Tanaka A, Kettunen H, Niskanen K and Keitaanniemi K 2000 *J. Pulp Pap. Sci.* **26** 385
[144] Tanaka A, Hiltunen E, Kettunen H and Niskanen K 2001 Fracture properties in filled papers *The Science of Papermaking, 12th Fundamental Research Symp. (Oxford, UK 17–21 September 2001)* vol 2, pp 1403–21
[145] Shallhorn P and Karnis A 1979 *Pulp Pap. Canada* **5** T92
Shallhorn P M 1994 *J. Pulp Pap. Sci.* **20** 119
[146] Maloney C and Lemaitre A 2004 *Phys. Rev. Lett.* **93** 016001
[147] Maloney C and Lemaitre A 2004 *Phys. Rev. Lett.* **93** 195501
[148] Kettunen H and Niskanen K 2000 *J. Pulp Pap. Sci.* **26** 35
Niskanen K, Kettunen H and Yu Y Damage width: a measure of the size of fracture process zone *The Science of Papermaking, 12th Fundamental Research Symp. (Oxford, UK 17–21 September 2001)* vol 2, pp 1467–82
[149] Duxbury P M, Beale P D and Leath P L 1986 *Phys. Rev. Lett.* **57** 1052
[150] Korteoja M, Salminen L I, Niskanen K J and Alava M 1998 *J. Pulp Pap. Sci.* **24** 1
[151] Zinck P, Pays M F, Rezhakhanlou R and Gerard J F 1999 *J. Mater. Sci.* **34** 2121
[152] Yamauchi T, Okumura S and Noguchi N 1990 *J. Pulp Pap. Sci.* **16** J44
[153] Gradin P A, Nyström S, Flink P, Forsberg S and Stollmaier F 1997 *J. Pulp Pap. Sci.* **23** J113
[154] Niskanen K J, Alava M J, Seppälä E T, Åström J 2000 *J. Pulp Pap. Sci.* **25** 167
[155] Zapperi S, Nukala P K and Simunovic S 2005 *Phys. Rev.* E **71** 026106
[156] Minozzi M, Caldarelli G, Pietronero L and Zapperi S 2003 *Eur. Phys. J.* B **36** 203
[157] Rosti J, Salminen L I and Alava M J *J. Pulp Pap. Sci.*
[158] Johansen A and Sornette D 2000 *Eur. Phys. J.* B **18** 163
[159] Salminen L I, Alava M J and Niskanen K J 2003 *Eur. Phys. J.* B **32** 369
[160] Mandelbrot B B, Passoja D E and Paullay A J 1984 *Nature (London)* **308** 721
[161] Engoy T, Maloy K J and Hansen A 1994 *Phys. Rev. Lett.* **73** 834
[162] Kertész J, Horvath V K and Weber F 1993 *Fractals* **1** 67
[163] Rosti J, Salminen L I, Seppälä E T, Alava M J and Niskanen K J 2001 *Eur. Phys. J.* B **19** 259
[164] Menezes-Sobrinho I L, Couto M S and Ribeiro I R B 2005 *Phys. Rev.* E **71** 066121
[165] Seppälä E T, Räisanen V I and Alava M J 2000 *Phys. Rev.* E **61** 6312
[166] Skejtne B, Helle T and Hansen A 2001 *Phys. Rev. Lett.* **87** 125503
[167] Kardar M, Parisi G and Zhang Y C 1986 *Phys. Rev. Lett.* **56** 889
[168] Bouchbinder E, Mathiesen J and Procaccia I 2004 *Phys. Rev. Lett.* **92** 245505
[169] Bouchaud E and Bouchaud J-P 1994 *Phys. Rev.* B **50** 17752
[170] Morel S, Schmittbuhl J, Bouchaud E and Valentin G 2000 *Phys. Rev. Lett.* **85** 1678
[171] Santucci S, Vanel L and Ciliberto S 2004 *Phys. Rev. Lett.* **93** 095505
[172] Balankin A S, Susarrey O and Bravo A 2001 *Phys. Rev.* E **64** 066131
[173] Alava M and Niskanen K 1997 Performance of reinforcement fibres in paper *The Fundamentals of Papermaking Materials, The Eleventh Fundamental Research Symp. (21–26 September 1997)* (Cambridge: Pira International) 1177–1213
[174] Koponen A, Kandhai D, Hellén E, Alava M, Hoekstra A, Kataja M, Niskanen K, Sloot P and Timonen J 1998 *Phys. Rev. Lett.* **80** 716
[175] Aaltosalmi U, Kataja M, Koponen A, Timonen J, Goel A, Lee G and Ramaswamy S 2004 *J. Pulp Pap. Sci.* **30** 251
[176] Qi D and Uesaka T 1996 *J. Mater. Sci.* **31** 4865
[177] Thompson K E 2002 *AICHE J.* **48** 1369
[178] Takahashi A, Häggkvist M and Li T Q 1997 *Phys. Rev.* E **56** 2035
[179] Bico J and Quéré D 2003 *Europhys. Lett.* **61** 348
[180] Siebold A, Nardin M, Schultz J and Walliser A 2000 *Colloid Surf.* A **161** 81
[181] Hamraoui A and Nylander T 2002 *J. Colloid Interface Sci.* **250** 415
[182] Pearson J R A and Tardy P M J 2002 *J. Non-Newton Fluid Mech.* **102** 447
[183] Tsakiroglou C D, Theodoropoulou M, Karoutsos V, Pananicolaou D and Sygouni V 2003 *J. Colloid Interface Sci.* **267** 217

[184] Aspler J 1993 *Nordic Pulp Pap. Res. J.* **1** 68
[185] Weir G J and White S P 1996 *Transp. Porous Media* **25** 79
[186] Gagnon R E, Parish G D and Bousfield D W 2001 *Tappi J.* **84** 66
[187] Bico J, Tordeux C and Quéré D 2001 *Europhys. Lett.* **55** 214
[188] Washburn E W 1921 *Phys. Rev.* **17** 273
[189] Aspler J S, Davis S and Lyne M B 1987 *J. Pulp Pap. Sci.* **13** J55
[190] Senden T J, Knackstedt M A and Lyne M B 2000 *Nordic Pulp Pap. Res. J.* **15** 554
[191] Schoelkopf J, Gane P A C, Ridgway C J and Matthews G P 2002 *Colloid Surf.* A **206** 445
[192] Bear J and Bachmat Y 1990 *Introduction to Modeling of Transport Phenomena in Porous Media* (Dordrecht: Kluwer)
[193] Blunt M, King M J and Scher H 1992 *Phys. Rev.* A **46** 7680
[194] Bernadiner M G 1998 *Transp. Porous Media* **30** 251
[195] Hughes R G and Blunt M J 2000 *Transp. Porous Media* **40** 295
[196] Blunt M J 2001 *Curr. Opin. Colloid Interface Sci.* **6** 197
[197] Hoyland R W 1976 *Trans. BPBIF Symp. Fiber-Water Interactions in Papermaking (Oxford)* pp 557–79
[198] See, e.g. Eklund D E and Salminen P J 1986 *Tappi J.* **69** 116
[199] Nederveen C J 1994 *Tappi J.* **77** 174
[200] Dubé M, Rost M, Elder K R, Alava M, Majaniemi S and Ala-Nissila T 1999 *Phys. Rev. Lett.* **83** 1628
[201] Dubé M, Rost M and Alava M 2000 *Eur. Phys. J.* B **15** 691
[202] Geromichalos D, Mugele F and Herminghaus S 2002 *Phys. Rev. Lett.* **89** 104503
[203] The paper of Koplik J and Levine H 1985 *Phys. Rev.* B **32** 280 implied that fluid invasion could be understood in terms of simple interfacial models, helping to catalyze activity in interfacial studies
[204] Horváth V K and Stanley H E 1995 *Phys. Rev.* E **52** 5166
[205] Kwon T H, Hopkins A E and O'Donnell S E 1996 *Phys. Rev.* E **54** 685
[206] Zik O, Moses E, Olami Z and Webman I 1997 *Europhys. Lett.* **38** 509
[207] Balankin A S, Bravo-Ortega A and Matamoros D M 2000 *Phil. Mag. Lett.* **80** 503
[208] Medina A, Pérez-Rosales C, Pineda A and Higuera F J 2001 *Rev. Mex. Fis.* **47** 537
[209] Dubé M, Chabot B, Daneault C and Alava M 2005 *Pulp Pap. Canada* **106** T178
Dubé M, Daneault C, Vuorinen V, Alava M and Rost M *J. Appl. Phys.* submitted
[210] See Anderson D M 2005 *Phys. Fluids* **17** 087104 and the references therein
[211] Chen K S A and Scriven L E 1990 *Tappi J.* **73** 151
[212] Marmur A 1992 *Adv. Colloid Interface Sci.* **39** 13
[213] Davis S H and Hocking L M 2000 *Phys. Fluids* **12** 1646
[214] Holman R K, Cima M J, Uhland S A and Sachs E 2002 *J. Colloid Interface Sci.* **249** 432
[215] Bazilevsky A V, Kornev K G, Rozhkov A N and Neimark A V 2003 *J. Colloid Interface Sci.* **262** 16